

1 **Thanatotranscriptome: genes actively expressed after** 2 **organismal death**

3
4 **Authors:** Alex E. Pozhitkov^{1,2}, Rafik Neme², Tomislav Domazet-Lošo^{3,4}, Brian G.
5 Leroux¹, Shivani Soni⁵, Diethard Tautz² and Peter A. Noble^{5,6,7*}.

6 **Affiliations:**

7 ¹Department of Oral Health Sciences, University of Washington, Box 357444, Seattle,
8 WA USA 98195.

9 ²Max-Planck-Institute for Evolutionary Biology, August-Thienemann-Strasse 2, 24306
10 Ploen, Germany.

11 ³Laboratory of Evolutionary Genetics, Division of Molecular Biology, Ruđer Bošković
12 Institute, 10002 Zagreb, Croatia.

13 ⁴Catholic University of Croatia, Ilica 242, Zagreb, Croatia.

14 ⁵Department of Periodontics, School of Dentistry, University of Washington, Box
15 357444, Seattle, WA USA 98195.

16 ⁶Department of Biological Sciences, Alabama State University, Montgomery, AL, USA
17 36101-0271.

18 ⁷PhD Program in Microbiology, Alabama State University, Montgomery, AL, USA
19 36101-0271.

20
21 *Correspondence to:

22 Peter A. Noble

23 Email: panoble@uwashington.edu

24 Phone: 206-409-6664.

25
26 AEP: pozhit@uw.edu

27 RN: rneme@evolbio.mpg.de

28 TDL: tdomazet@unicath.hr

29 BGL: leroux@uw.edu

30 SS: ssoni@alasu.edu

31 DT: tautz@evolbio.mpg.edu

32
33 **Short Title:** Transcriptional dynamics after organismal death

34

35 **ABSTRACT**

36 A continuing enigma in the study of biological systems is what happens to highly ordered
37 structures, far from equilibrium, when their regulatory systems suddenly become
38 disabled. In life, genetic and epigenetic networks precisely coordinate the expression of
39 genes -- but in death, it is not known if gene expression diminishes gradually or abruptly
40 stops or if specific genes are involved. We investigated the ‘unwinding of the clock’ by
41 identifying upregulated genes, assessing their functions, and comparing their
42 transcriptional profiles through postmortem time in two species, mouse and zebrafish.
43 We found transcriptional abundance profiles of 1,063 genes were significantly changed
44 after death of healthy adult animals in a time series spanning from life to 48 or 96 h
45 postmortem. Ordination plots revealed non-random patterns in profiles by time. While
46 most thanatotranscriptome (thanatos-, Greek *defn.* death) transcript levels increased
47 within 0.5 h postmortem, some increased only at 24 and 48 h. Functional
48 characterization of the most abundant transcripts revealed the following categories:
49 stress, immunity, inflammation, apoptosis, transport, development, epigenetic regulation,
50 and cancer. The increase of transcript abundance was presumably due to thermodynamic
51 and kinetic controls encountered such as the activation of epigenetic modification genes
52 responsible for unraveling the nucleosomes, which enabled transcription of previously
53 silenced genes (e.g., development genes). The fact that new molecules were synthesized
54 at 48 to 96 h postmortem suggests sufficient energy and resources to maintain self-
55 organizing processes. A step-wise shutdown occurs in organismal death that is
56 manifested by the apparent upregulation of genes with various abundance maxima and
57 durations. The results are of significance to transplantology and molecular biology.

58 **KEYWORDS**

59 Postmortem transcriptome; postmortem gene expression; Gene meters; calibrated DNA
60 microarrays, thanatotranscriptome; cancer; signaling, development, immunity, apoptosis,
61 transport, inflammation; epigenetic regulation; thermodynamic sink; transplantology,
62 forensic science.

63

64 INTRODUCTION

65 A healthy adult vertebrate is a complex biological system capable of highly elaborate
66 functions such as the ability to move, communicate, and sense the environment -- all at
67 the same time. These functions are tightly regulated by genetic and epigenetic networks
68 through multiple feedback loops that precisely coordinate the expression of thousands of
69 genes at the right time, in the right place, and in the right level [1]. Together, these
70 networks maintain homeostasis and thus sustain 'life' of a biological system.

71 While much is known about gene expression circuits in life, there is a paucity of
72 information about what happens to these circuits after organismal death. For example, it
73 is not well known whether gene expression diminishes gradually or abruptly stops in
74 death -- nor whether specific genes are newly expressed or upregulated. In organismal
75 'death', defined here as the cessation of the highly elaborate system functions in
76 vertebrates, we conjecture that there is a gradual disengagement and loss of global
77 regulatory networks, but this could result in a regulatory response of genes involved in
78 survival and stress compensation. To test this, we examined postmortem gene expression
79 in two model organisms: the zebrafish, *Danio rerio*, and the house mouse, *Mus musculus*.
80 The purpose of the research was to investigate the "unwinding of the clock" by
81 identifying genes whose expression increases (i.e., nominally upregulated) and assessing
82 their functions based on the primary literature. The biological systems investigated in
83 this study are different from those examined in other studies, such as individual dead
84 and/or injured cells in live organisms, i.e., apoptosis and necrosis (reviewed in refs. [2-
85 5]). In contrast to previous studies, gene expression from the entire *D. rerio* body, and
86 the brains and livers of *M. musculus* were assessed through postmortem time. Gene
87 expression was measured using the 'Gene Meter' approach that precisely reports gene
88 transcript abundances based on a calibration curve for each microarray probe [6].

89 MATERIALS AND METHODS

90 **Induced death and postmortem incubation.** Zebrafish Forty-four female *Danio rerio*
91 were transferred from several flow-through aquaria kept at 28°C to a glass beaker
92 containing 1 L of aquarium water. Four individuals were immediately taken out, snap
93 frozen in liquid nitrogen, and stored in Falcon tubes at -80°C (two zebrafish per tube).
94 These samples were designated as the first set of live controls. A second set of live
95 controls was immersed in an open cylinder (described below). Two sets of live controls
96 were used to determine if putting the zebrafish back into their native environment had
97 any effects on gene expression (we later discovered no significant effects).

98 The rest of the zebrafish were subjected to sudden death by immersion in a "kill"
99 chamber. The chamber consisted of an 8 L styrofoam container filled with chilled ice
100 water. To synchronize the death of the rest of the zebrafish, they were transferred to an
101 open cylinder with a mesh-covered bottom and the cylinder was immersed into the kill
102 chamber. After 20 to 30 s of immersion, four zebrafish were retrieved from the chamber,
103 snap frozen in liquid nitrogen, and stored at -80°C (two zebrafish per Falcon tube). These
104 samples were designated as the second set of live controls. The remaining zebrafish were

105 kept in the kill chamber for 5 min and then the cylinder was transferred to a flow-through
106 aquarium kept at 28°C so that they were returned to their native environment.

107 Postmortem sampling of the zebrafish occurred at: time 0, 15 min, 30 min, 1 h, 4 h, 8 h,
108 12 h, 24 h, 48 h, and 96 h. For each sampling time, four expired zebrafish were retrieved
109 from the cylinder, snap frozen in liquid nitrogen, and stored at -80°C in Falcon tubes (two
110 zebrafish to a tube). One zebrafish sample was lost, but extraction volumes were
111 adjusted to one organism.

112 Mouse The mouse strain C57BL/6JRj (Janvier SAS, France) was used for our
113 experiments. The mice were 20-week old males of approximately the same weight. The
114 mice were highly inbred and were expected to have a homogenous genetic background.
115 Prior to euthanasia, the mice were kept at room temperature and were given *ad libitum*
116 access to food and water. Each mouse was euthanized by cervical dislocation and placed
117 in an individual plastic bag with holes to allow air / gas exchange. The bagged carcasses
118 were kept at room temperature in a large, open polystyrene container. Sampling of the
119 deceased mice began at 0 h (postmortem time zero) and continued at 30 min, 1 h, 6 h, 12
120 h, 24 h and 48 h postmortem. At each sample time, 3 mice were sampled (except for 48h
121 where 2 mice were sampled) and the entire brain (plus stem) and two portions of the liver
122 were extracted from each mouse. For liver samples, clippings were taken from the
123 foremost and rightmost lobes of the liver. The brain and liver samples were snap frozen
124 in liquid nitrogen and stored individually in Falcon tubes at -80°C.

125 The euthanasia methods outlined above are approved by the American Veterinary
126 Medical Association (AVMA) Guidelines for Euthanasia (www.avma.org) and carried
127 out by personnel of the Max-Planck-Institute for Evolutionary Biology (Ploen, Germany).
128 All animal work: followed the legal requirements, was registered under number V312-
129 72241.123-34 (97-8/07) and approved by the ethics commission of the Ministerium für
130 Landwirtschaft, Umwelt und ländliche Räume, Kiel (Germany) on 27. 12. 2007.

131 **RNA extraction, labeling, hybridization and DNA microarrays.** The number of
132 biologically distinct organisms was 43 for zebrafish and 20 for mice. Samples from two
133 fish were pooled for analysis, resulting in two replicate measurements at each time point.
134 The number of replicated measurements for mice was three at each of the first six time
135 points and two at 48h. Thus, the total number of samples analyzed was 22 for zebrafish
136 and 20 for mice. For the zebrafish, samples were mixed with 20 ml of Trizol and
137 homogenized using a TissueLyzer (Qiagen). For the mice, 100 mg of brain or liver
138 samples were mixed with 1 ml of Trizol and homogenized. One ml of the emulsion from
139 each sample was put into a fresh 1.5 ml centrifuge tube for RNA extraction and the rest
140 was frozen at -80°C.

141 RNA was extracted by adding 200 µl of chloroform, vortexing the sample, and
142 incubating it at 25°C for 3 min. After centrifugation (15 min at 12000 x g at 4°C), the
143 supernatant (approx. 350 µl) was transferred to a fresh 1.5 ml tube containing an equal
144 volume of 70% ethanol. The tube was vortexed, centrifuged and purified following the
145 procedures outlined in the PureLink RNA Mini Kit (Life Technologies, USA).

146 The isolated RNA, 400 ng per sample, was labeled, purified and hybridized according to
147 the One-Color Microarray-based Gene Expression Analysis (Quick Amp Labeling) with
148 Tecan HS Pro Hybridization kit (Agilent Technologies). For the zebrafish, the labeled

149 RNA was hybridized to the Zebrafish (v2) Gene Expression Microarray (Design ID
150 019161). For the mouse, the labeled RNA was hybridized to the SurePrint G3 Mouse GE
151 8x60K Microarray Design ID 028005 (Agilent Technologies). The microarrays were
152 loaded with 1.65 μg of labeled cRNA for each postmortem sample.

153 **Microarray calibration.** Oligonucleotide (60 nt) probes on the zebrafish and mouse
154 microarrays were calibrated using pooled labeled cRNA of all zebrafish and all mouse
155 postmortem samples, respectively. The dilution series for the Zebrafish array was created
156 using the following concentrations of labeled cRNA: 0.41, 0.83, 1.66, 1.66, 1.66, 3.29,
157 6.60, and 8.26 μg . The dilution series for the Mouse arrays was created using the
158 following concentrations of labeled cRNA: 0.17, 0.33, 0.66, 1.32, 2.64, 5.28, 7.92, and
159 10.40 μg . Calibration involved plotting the signal intensities of the probes against a
160 dilution factor and determining the isotherm model (e.g., Freundlich and/or Langmuir)
161 that best fit the relationship between signal intensities and gene abundances.

162 Consider zebrafish gene transcripts targeted by A_15_P110618 (which happens to be one
163 of the transcriptional profiles of gene *Hsp70.3* shown in Fig 2A). External file
164 FishProbesParameters.txt shows that a Freundlich model best fit the dilution curve with
165 $R^2=0.99$. The equation for this probe is the following:

$$166 \quad SI = \exp(7.1081)x^{0.67632}$$

167 where SI is the observed average signal intensity for dilution x . The gene abundance G
168 was calculated by inverting this equation. For this probe, signal intensity at each
169 postmortem time, SI_t , is determined by the equation: $G = (SI_t / \exp(7.1081))^{1/0.67632}$.
170 Specifically, consider two biological replicates of 15 min postmortem zebrafish, the
171 signal intensities of the probe A_15_P110618 are 770.5 and 576.0, which translates into
172 the abundances 0.50 and 0.33 arbitrary units (a.u.) respectively. The target abundances
173 were further converted to log10 and are shown in external file Fish_log10_AllProfiles.txt.

174 Details of the calibration protocols to calculate gene expression values, i.e., mRNA
175 relative abundances, are provided in our recent paper where we describe the “Gene
176 Meter” [6].

177 **Statistical analysis.** Abundance levels were log-transformed for analysis to stabilize the
178 variance. A one-sided Dunnett’s T-statistic was applied to test for increase at one or more
179 postmortem times compared to live control (fish) or time 0 (mouse). A bootstrap
180 procedure with 10^9 simulations was used to determine the critical value for the Dunnett
181 statistics in order to accommodate departures from parametric assumptions and to
182 account for multiplicity of testing. The profiles for each gene were centered by
183 subtracting the mean values at each postmortem time point to create “null” profiles.
184 Bootstrap samples of the null profiles were generated to determine the 95th percentile of
185 the maximum (over all genes) of the Dunnett statistics. Significant postmortem
186 upregulated genes were selected as those having Dunnett T values larger than the 95th
187 percentile. Only significantly upregulated genes were retained for further analyses.

188 Orthogonal transformation of the abundances to their principal components (PC) was
189 conducted and the results were graphed on a 2 dimensional ordination plot. The $m \times n$
190 matrix of abundances (sampling times by number of gene transcripts), which is 10×548
191 for zebrafish and 7×515 for mouse, was used to produce an $m \times m$ matrix D of Euclidean

192 distances between all pairs of sampling times. Principal component analysis (PCA) was
193 performed on the matrix of distances, D. To investigate and visualize differences
194 between the sampling times, a scatterplot of the first two principal components (PC1 and
195 PC2) was created. To establish relative contributions of the gene transcripts, the
196 projection of each sampling time onto the (PC1, PC2) plane was calculated and those
197 genes with high correlations (≥ 0.70) between abundances and either component (PC1 or
198 PC2) were displayed as a biplot.

199 **Gene annotation and functional categorization.** Microarray probe sequences were
200 individually annotated by performing a BLASTN search of the zebrafish and mouse
201 NCBI databases (February, 2015). The gene annotations were retained if the bit score
202 was greater than or equal to 100 and the annotations were in the correct 5' to 3'
203 orientation. Transcription factors, transcriptional regulators, and cell signaling
204 components (e.g., receptors, enzymes, and messengers) were identified as global
205 regulatory genes. The rest were considered response genes.

206 Functional categorizations were performed by querying the annotated gene transcripts in
207 the primary literature and using UniProt (www.uniprot.org). Genes not functionally
208 categorized to their native organism (zebrafish or mouse) were categorized to genes of
209 phylogenetically related organisms (e.g., human). Cancer-related genes were identified
210 using a previously constructed database (see Additional File 1: Table S1 in [7]).

211

212 **RESULTS**

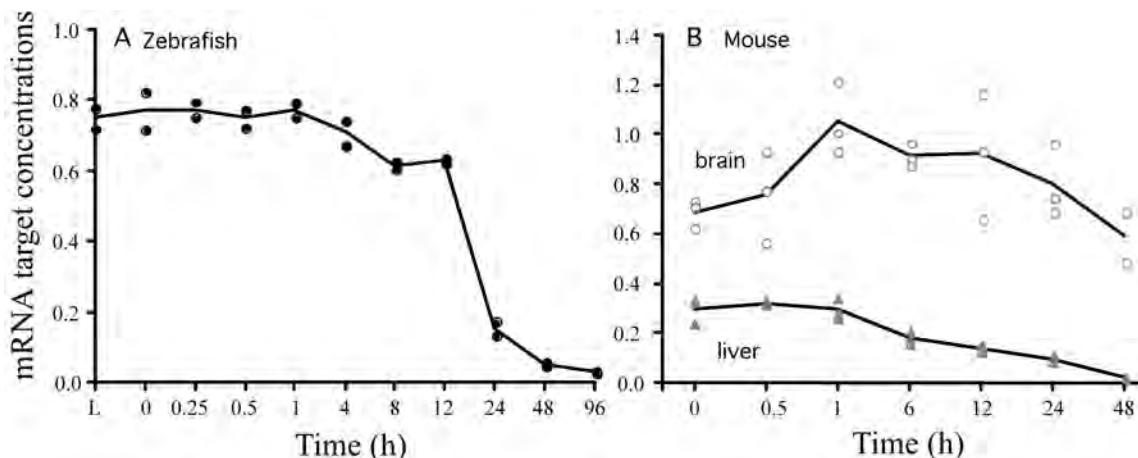
213 Similar quantities of total mRNA were extracted from zebrafish samples for the first 12 h
214 postmortem (avg. 1551 ng per μ l tissue extract) then the quantities abruptly decreased
215 with postmortem time (Table S1). The quantities of total mRNA extracted from the
216 mouse liver samples were about the same for the first 12 h postmortem (avg. of 553 ng
217 per μ l tissue extract) then they increased with time (Table S2). The quantities of total
218 mRNA extracted from the mouse brain samples were similar (avg. of 287 ng per μ l tissue
219 extract) for all postmortem times (Table S2). Hence, the amount of total mRNA
220 extracted depended of the organism/organ/tissue and time.

221 Calibration of the microarray probes and determination of the transcript abundances at
222 each postmortem sampling time produced a fine-grain series of data for the zebrafish and
223 the mouse. Approximately 84.3% (36,811 of 43,663) zebrafish probes and 67.1%
224 (37,368 of 55,681) mouse probes were found to provide a suitable dose-response curve
225 for calibration (data available upon request).

226 Figure 1 shows the sum of all gene abundances calculated from the calibrated probes with
227 postmortem time. In general, the sum of all abundances decreased with time, which
228 means that less targets hybridized to the microarray probes. In the zebrafish, mRNA
229 decreased abruptly at 12 h postmortem (Fig 1A), while for the mouse brain Fig 1B), total
230 mRNA increased in the first hour and then gradually decreased. For the mouse liver,
231 mRNA gradually decreased with postmortem time. The fact that total mRNA shown in
232 Figs 1A and 1B mirrors the electrophoresis banding patterns shown in Fig S1 and S2
233 (ignoring the 28S and 18S rRNA bands) indicates a general agreement of the Gene Meter

234 approach to another molecular approach (i.e., Agilent Bioanalyzer). Hence, total mRNA
235 abundances depended on the organism (zebrafish, mouse), organ (brain, liver), and
236 postmortem time, which are aligned with previous studies [8,9,10,11,12,13].

237



238

239

240

241

242

243

Fig 1. Total mRNA abundance (arbitrary units, a.u.) by postmortem time determined using all calibrated microarray probes. A, extracted from whole zebrafish; B, extracted from brain and liver tissues of whole mice. Each datum point represents the mRNA from two organisms in the zebrafish and a single organism in the mouse.

244

245

246

247

248

249

250

251

252

253

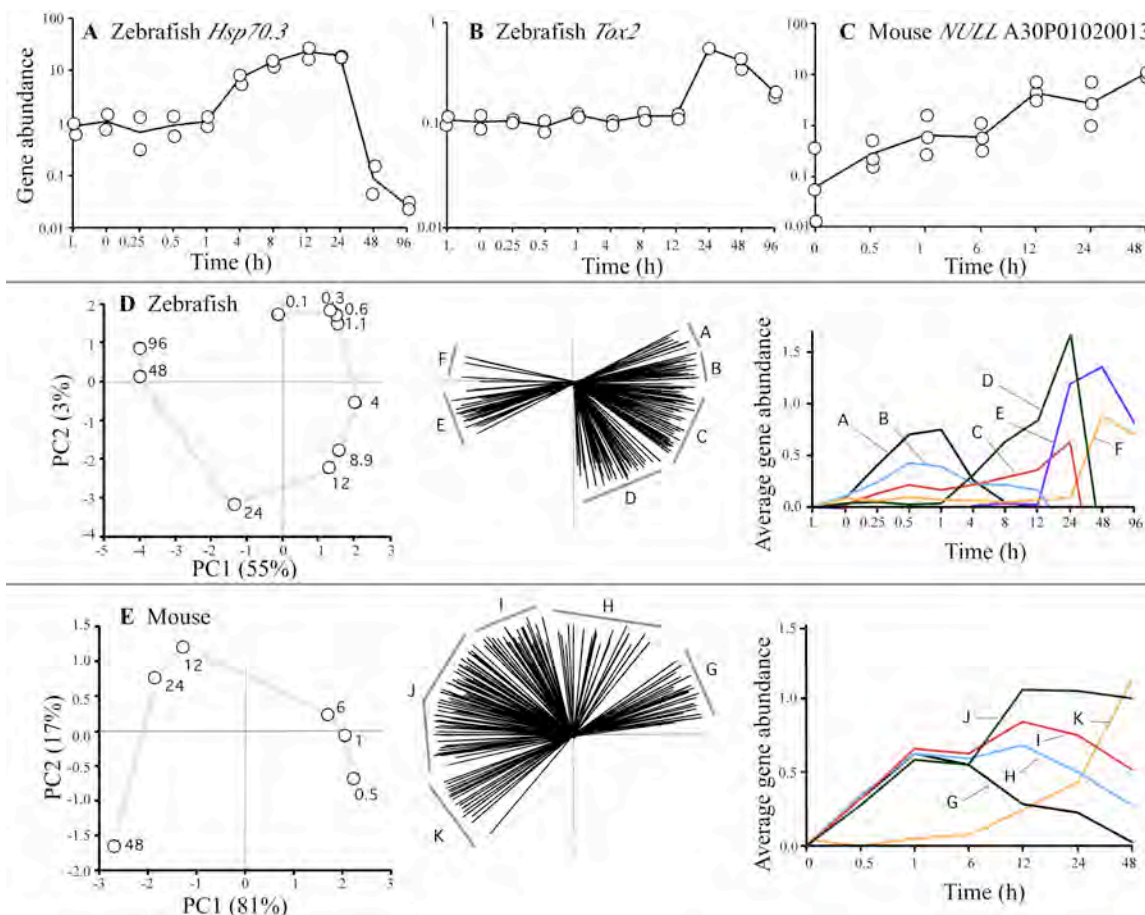
254

255

256

The abundance of a gene transcript is determined by its rate of synthesis and its rate of degradation [14]. We focused on genes that show a significant increase in RNA abundance -- relative to live controls -- because these genes are likely to be actively transcribed in organismal death despite an overall decrease in total mRNA with time. An upregulated transcription profile was defined as one having at least one time point where the abundance was statistically higher than that of the control (Fig 2 A to 2C). It is important to understand that the entire profiles, i.e., 22 data points for the zebrafish and 20 points for the mouse, were subjected to a statistical test to determine significance (see Materials and Methods). We found 548 zebrafish transcriptional profiles and 515 mouse profiles were significantly upregulated. The fact that there are upregulated genes is consistent with the notion that there is still sufficient energy and functional cellular machinery for transcription to occur -- long after organismal death.

256



257

258

259

260

261

262

263

264

265

266

267

268

269

270

271

272

273

274

275

276

277

Fig 2. Transcriptional profiles of representative genes (a.u.), ordination plots based on transcript abundances by postmortem time (h) with corresponding transcript contributions (biplots), and averaged transcript abundances by group. (A) Transcriptional profile of the *Hsp70.3* gene, (B) the *Tox2* gene, and (C) the NULL (i.e., no annotation, probe number shown) gene as a function of postmortem time. Each datum point was derived from the mRNA of two zebrafish or one mouse. (D) Ordination plots of the zebrafish and (E) mouse were based on all upregulated gene profiles by postmortem time (h). Gene transcripts in the biplots were arbitrarily assigned alphabetical groups based on their positions in the ordination. The average transcript abundances for each group are shown.

Based on GenBank gene annotations, we found that among the upregulated genes for the zebrafish, 291 were protein-coding genes (53%) and 257 non-coding mRNA (47%) and, for the mouse, 324 known protein-coding genes (63%), 190 non-coding mRNA (37%), and one control sequence of unknown composition. Hence, about 58% of the total upregulated genes in the zebrafish and mouse are known and the rest (42%) are non-coding RNA.

Examples of genes yielding transcripts that significantly increased in abundance with postmortem time are: the ‘Heat shock protein’ (*Hsp70.3*) gene, the ‘Thymocyte selection-associated high mobility group box 2’ (*Tox2*) gene, and an unknown (*NULL*) gene (Fig

278 2A to 2C). While the *Hsp70.3* transcript increased after 1 h postmortem to reach a
279 maximum at 12 h, the *Tox2* transcript increased after 12 h postmortem to reach a
280 maximum at 24 h, and the *NULL* transcript consistently increased with postmortem time.
281 These figures provide typical examples of transcript profiles and depict the high
282 reproducibility of the sample replicates as well as the quality of output obtained using the
283 Gene Meter approach.

284 **Non-random patterns in transcript profiles**

285 Ordination plots of the significantly upregulated transcript profiles revealed prominent
286 differences with postmortem time (Fig 2D and 2E), suggesting the expression of genes
287 followed a discernible (non-random) pattern in both organisms. The biplots showed that
288 203 zebrafish transcript profiles and 226 mouse profiles significantly contributed to the
289 ordinations. To identify patterns in the transcript profiles, we assigned them to groups
290 based on their position in the biplots. Six profile groups were assigned for the zebrafish
291 (A to F) and five groups (G to K) were assigned for the mouse. Determination of the
292 average gene transcript abundances by group revealed differences in the shapes of the
293 averaged profiles, particularly the timing and magnitude of peak transcript abundances,
294 which accounted for the positioning of data points in the ordinations.

295 Genes coding for global regulatory functions were examined separately from others (i.e.,
296 response genes). Combined results show that about 33% of the upregulated genes in the
297 ordination plots were involved in global regulation with 14% of these encoding
298 transcription factors/transcriptional regulators and 19% encoding cell signaling proteins
299 such as enzymes, messengers, and receptors (Table S3). The response genes accounted
300 for 67% of the upregulated transcripts.

301 The genes were assigned to 22 categories (File S8) with some genes having multiple
302 categorizations. For example, the Eukaryotic Translation Initiation Factor 3 Subunit J-B
303 (*Eif3j2*) gene was assigned to protein synthesis and cancer categories [15].

304 Genes in the following functional categories were investigated: stress, immunity,
305 inflammation, apoptosis, solute/ion/protein transport, embryonic development, epigenetic
306 regulation and cancer. We focused on these categories because they were common to
307 both organisms and contained multiple genes, and they might provide explanations for
308 postmortem upregulation of genes (e.g., epigenetic gene regulation, embryonic
309 development, cancer). The transcriptional profiles of the genes were plotted by category
310 and each profile was ordered by the timing of the upregulation and peak transcript
311 abundance. This allowed comparisons of gene expression dynamics as a function of
312 postmortem time for both organisms. For each category, we provided the gene name and
313 function and compared expression dynamics within and between the organisms.

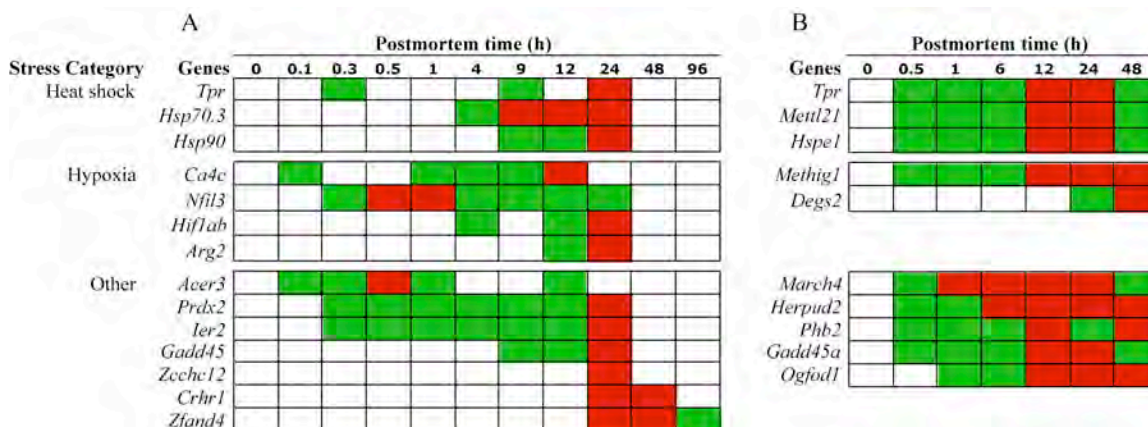
314 **Stress response**

315 In organismal death, we anticipated the upregulation of stress response genes because
316 these genes are activated in life to cope with perturbations and to recover homeostasis
317 [16]. The stress response genes were assigned to three groups: heat shock protein (*Hsp*),
318 hypoxia-related, and 'other' responses such as oxidative stress.

319 **Hsp** In the zebrafish, upregulated *Hsp* genes included: ‘Translocated promoter region’
 320 (*Tpr*), *Hsp70.3*, and *Hsp90* (Fig 3). The *Tpr* gene encodes a protein that facilitates the
 321 export of the *Hsp* mRNA across the nuclear membrane [17] and has been implicated in
 322 chromatin organization, regulation of transcription, mitosis [18] and controlling cellular
 323 senescence [19]. The *Hsp70.3* and *Hsp90* genes encode proteins that control the level of
 324 intracellular calcium [20], assist with protein folding, and aid in protein degradation [21].

325 In the mouse, upregulated *Hsp* genes included: *Tpr*, *Hsp*-associated methyltransferase
 326 (*Mettl21*) and Heat Shock Protein 1 (*Hspe1*) (Fig 3). The *Mettl21* gene encodes a protein
 327 modulating *Hsp* functions [22]. The *Hspe1* gene encodes a chaperonin protein that
 328 assists with protein folding in the mitochondria [23].

329 The timing and duration of *Hsp* upregulation varied by organism. In general, activation
 330 of *Hsp* genes occurred much later in the zebrafish than the mouse (4 h vs. 0.5 h
 331 postmortem, respectively). There were also differences in transcript abundance maxima
 332 since, in the zebrafish, maxima were reached at 9 to 24 h, while in the mouse maxima
 333 were reached at 12 to 24 h. Previous studies have examined the upregulation of *Hsp70.3*
 334 with time in live serum-stimulated human cell lines [24]. In both the zebrafish and
 335 human cell lines the *Hsp70.3* gene transcript reached maximum abundance at about 12 h
 336 (Fig 2A), indicating the same reactions are occurring in life and death.



337

338 **Fig 3. Upregulated stress response genes by postmortem time (h) and stress**
 339 **category. A. zebrafish; B, mouse. Green, intermediate value; Red, maximum value.**

340

341 **Hypoxia**

342 In the zebrafish, upregulated hypoxia-related genes included: Carbonic anhydrase 4
 343 (*Ca4c*), Nuclear factor interleukin-3 (*Nfil3*), Hypoxia-inducible factor 1-alpha (*Hif1ab*)
 344 and Arginase-2 (*Arg2*) (Fig 3). The Carbonic anhydrase 4 (*Ca4c*) gene encodes an
 345 enzyme that converts carbon dioxide into bicarbonate in response to anoxic conditions
 346 [25]. The *Nfil3* gene encodes a protein that suppresses hypoxia-induced apoptosis [26]
 347 and activates immune responses [27]. The *Hif1ab* gene encodes a transcription factor that
 348 prepares cells for decreased oxygen [28]. The *Arg2* gene encodes an enzyme that
 349 catalyzes the conversion of arginine to urea under hypoxic conditions [29]. Of note, the
 350 accumulation of urea presumably triggered the upregulation of the *Slc14a2* gene at 24 h,
 351 reported in the Transport Section (below).

352 In the mouse, upregulated hypoxia genes included: Methyltransferase hypoxia inducible
353 domain (*Methig1*) and Sphingolipid delta-desaturase (*Degs2*) (Fig 3). The *Methig1* gene
354 encodes methyltransferase that presumably is involved in gene regulation [30]. The
355 *Degs2* gene encodes a protein that acts as an oxygen sensor and regulates ceramide
356 metabolism [31]. Ceramides are waxy lipid molecules in cellular membranes that
357 regulate cell growth, death, senescence, adhesion, migration, inflammation, angiogenesis
358 and intracellular trafficking [32].

359 The activation of the *Ca4c* gene in the zebrafish indicates a build up of carbon dioxide at
360 0.1 to 1 h postmortem in the zebrafish presumably due lack of blood circulation. The
361 upregulation of the *Nfil3* gene in the zebrafish and *Methig1* gene in the mouse suggests
362 hypoxic conditions existed within 0.5 h postmortem in both organisms. The upregulation
363 of other hypoxia genes varied with postmortem time, with the upregulation of *Hiflab*,
364 *Arg2*, and *Degs2* genes occurring at 4 h, 12 h and 24, respectively.

365 **Other stress responses**

366 In the zebrafish, upregulated response genes included: Alkaline ceramidase 3 (*Acer3*),
367 Peroxiredoxin 2 (*Prdx2*), Immediate early (*Ier2*), Growth arrest and DNA-damage-
368 inducible protein (*Gadd45a*), Zinc finger CCH domain containing 12 (*Zcchc12*),
369 Corticotropin releasing hormone receptor 1 (*Crhr1*), and Zinc finger AN1-type domain 4
370 (*Zfand4*) (Fig 3). The *Acer3* gene encodes a stress sensor protein that mediates cell-
371 growth arrest and apoptosis [33]. The *Prdx2* gene encodes an antioxidant enzyme that
372 controls peroxide levels in cells [34] and triggers production of *Tnfa* proteins that induce
373 inflammation [35]. The *Ier2* gene encodes a transcription factor involved in stress
374 response [36]. The *Gadd45a* gene encodes a stress protein sensor that stops the cell cycle
375 [37], modulates cell death and survival, and is part of the signaling networks in immune
376 cells [38]. The *Zcchc12* gene encodes a protein involved in stress response in the brain
377 [39]. The *Crhr1* and *Zfand4* genes encode stress proteins [40,41].

378 While the *Acer3*, *Prdx2*, and *Ier2* genes were activated within 0.3 h postmortem,
379 indicating a changed physiological state; the *Gadd45a* gene was activated at 9 h and the
380 other genes (*Zcchc12*, *Crhr1*, *Zfand4*) were activated at 24 h postmortem.

381 In the mouse, upregulated stress response genes included: Membrane-associated RING-
382 CH 4 (*March4*), Homocysteine-responsive endoplasmic reticulum-resident ubiquitin-like
383 domain member 2 (*Herpud2*), Prohibitin-2 (*Phb2*), *Gadd45a*, and Two-oxoglutarate and
384 iron-dependent oxygenase domain-containing 1 (*Ogfod1*) (Fig 3). The *March4* gene
385 encodes an immunologically-active stress response protein [42]. The *Herpud2* gene
386 encodes a protein that senses the accumulation of unfolded proteins in the endoplasmic
387 reticulum [43]. The *Phb2* gene encodes a cell surface receptor that responds to
388 mitochondrial stress [44]. The *Ogfod1* gene encodes a stress-sensing protein [45].

389 Note that the stress genes in the mouse were all activated within 1 h postmortem and
390 remained upregulated for 48 h.

391 **Summary of stress response**

392 In both organisms, organismal death activated heat shock, hypoxia, and other stress
393 genes, which varied in the timing and duration of upregulation within and between
394 organisms. Consider, for example, the *Tpr* and *Gadd45a* genes, which were common to
395 both organisms. While the *Tpr* genes were upregulated within 0.5 h postmortem in both

396 organisms, the *Gadd45a* gene was upregulated at 9 h in the zebrafish and 0.5 h in the
397 mouse. In addition, the transcription profile of the *Tpr* gene was more variable in the
398 zebrafish than the mouse since it was activated at 0.3 h, 9 h and 24 h postmortem, which
399 suggest the gene might be regulated through a feedback loop. In contrast, in the mouse,
400 the *Tpr* gene was upregulated at 0.5 h and the transcripts reached peak abundance at 12
401 and 24 h postmortem.

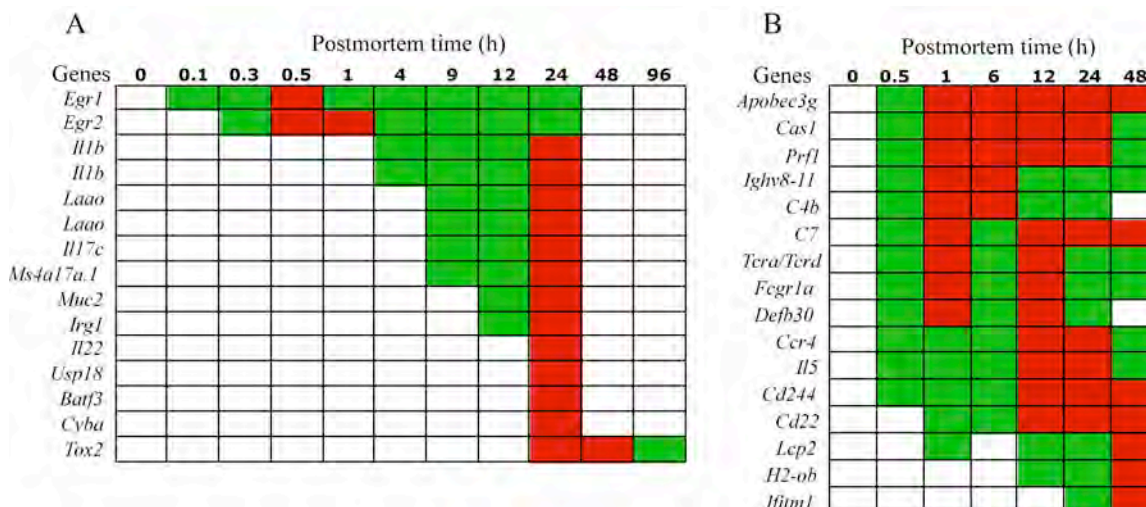
402 Taken together, the stress genes were activated in both organisms to compensate for a
403 loss in homeostasis.

404 **Innate and adaptive immune responses**

405 In organismal death, we anticipated the upregulation of immune response genes because
406 vertebrates have evolved ways to protect the host against infection in life, even under
407 absolutely sterile conditions [46]. Inflammation genes were excluded from this section
408 (even though they are innate immune genes) because we examined them in a separate
409 section (below).

410 In the zebrafish, upregulated immunity genes included: Early growth response-1 and -2
411 (*Egr1*, *Egr2*), Interleukin-1b (*Il1b*), L-amino acid oxidase (*Lao*), Interleukin-17c (*Il17c*),
412 Membrane-spanning 4-domains subfamily A member 17A.1 (*Ms4a17.a1*), Mucin-2
413 (*Muc2*), Immunoresponsive gene 1 (*Irg1*), Interleukin- 22 (*Il22*), Ubl carboxyl-terminal
414 hydrolase 18 (*Usp18*), ATF-like 3 (*Batf3*), Cytochrome b-245 light chain (*Cyba*), and
415 “Thymocyte selection-associated high mobility group” box protein family member 2
416 (*Tox2*) (Fig 4). The *Egr1* and *Egr2* genes encode proteins that regulate B and T cell
417 functions in adaptive immunity [47,48]. The *Il1b* gene encodes an interleukin that kills
418 bacterial cells through the recruitment of other antimicrobial molecules [49]. The *Lao*
419 gene encodes an oxidase involved in innate immunity [50]. The *Il17c* and *Il22* genes
420 encode interleukins that work synergically to produce antibacterial peptides [51]. The
421 *Ms4a17.a1* gene encodes a protein involved in adaptive immunity [52]. The *Muc2* gene
422 encodes a protein that protects the intestinal epithelium from pathogenic bacteria [53].
423 The *Irg1* gene encodes an enzyme that produces itaconic acid, which has antimicrobial
424 properties [54]. The *Usp18* gene encodes a protease that plays a role in adaptive
425 immunity [55]. The *Batf3* gene encodes a transcription factor that activates genes
426 involved in adaptive immunity [56]. The *Cyba* gene encodes an oxidase that is used to
427 kill microorganisms [57]. The *Tox2* gene encodes a transcription factor that regulates
428 Natural Killer (NK) cells of the innate immune system [58].

429



430

431 **Fig 4. Upregulated immunity genes by postmortem time (h). A. zebrafish; B, mouse.**

432 **Green, intermediate value; Red, maximum value. Some transcripts were**

433 **represented by two different probes (e.g. *Il1b*, *Laoa*).**

434

435 Upregulation of immunity genes in the zebrafish occurred at different times with varying
 436 durations. While genes involved in adaptive immunity were upregulated at 0.1 to 0.3 h
 437 (*Egr*), 9 h (*Ms4a17.a1*) and 24 h (*Usp18*, *Batf3*) postmortem, genes involved in innate
 438 immunity were upregulated at 4 h (*Il1b*), 9 h (*Laoa*, *Il17c*), 12 h (*Muc2*, *Irg1*) and 24 h
 439 (*Il22*, *Cyba*, *Tox2*) indicating a multi-pronged and progressive approach to deal with
 440 injury and the potential of microbial invasion.

441 In the mouse, upregulated antimicrobial genes included: Catalytic polypeptide-like 3G
 442 (*Apobec3g*), CRISPR-associated endonuclease (*Cas1*), Perforin-1 (*Prf1*),
 443 Immunoglobulin heavy variable 8-11 (*Ighv8-11*), C4b-binding protein (*C4b*),
 444 Complement component C7 (*C7*), T cell receptor alpha and delta chain (*Tcra/Tcrd*), High
 445 affinity immunoglobulin gamma Fc receptor I (*Fcgr1a*), Defensin (*Defb30*), Chemokine-
 446 4 (*Ccr4*), Interleukin-5 (*Il5*), NK cell receptor 2B4 (*Cd244*), Cluster of differentiation-22
 447 (*Cd22*), Lymphocyte cytosolic protein 2 (*Lcp2*), Histocompatibility 2 O region beta locus
 448 (*H2ob*) and Interferon-induced transmembrane protein 1 (*Ifitm1*) (Fig 4). The *Apobec3g*
 449 gene encodes a protein that plays a role in innate anti-viral immunity [59]. The *Cas1*
 450 gene encodes a protein involved in regulating the activation of immune systems
 451 [60,61,62,63]. The *Prf1*, *C7*, and *Defb30* genes encode proteins that kill bacteria by
 452 forming pores in the plasma membrane of target cells [64,65,66]. The *Ighv8-11* gene
 453 encodes an immunoglobulin of uncertain function. The *C4b* gene encodes a protein
 454 involved in the complement system [67]. The *Tcra/Tcrd* genes encode proteins that play
 455 a role in the immune response [68]. The *Fcgr1a* gene encodes a protein involved in both
 456 innate and adaptive immune responses [69]. The *Ccr4* gene encodes a cytokine that
 457 attracts leukocytes to sites of infection [70]. The *Il5* gene encodes an interleukin
 458 involved in both innate and adaptive immunity [71,72]. The *Cd244* and *Cd22* genes
 459 encode proteins involved in innate immunity [73]. The *Lcp2* gene encodes a signal-
 460 transducing adaptor protein involved in T cell development and activation [74]. The

461 *H2ob* gene encodes a protein involved in adaptive immunity. The *Ifitm1* gene encodes a
 462 protein that has antiviral properties [75].

463 Most immune response genes were upregulated within 1 h postmortem in the mouse
 464 ($n=14$ out of 16 genes), indicating a more rapid response than that of the zebrafish.

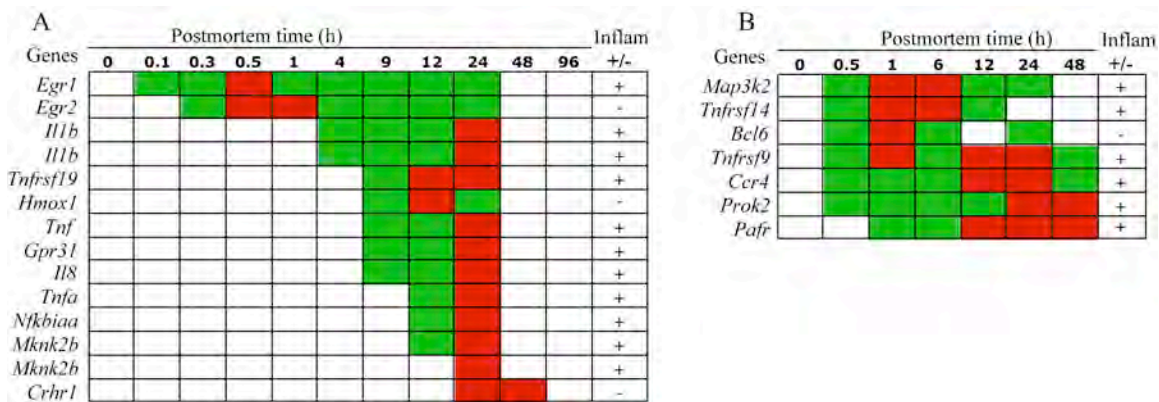
465 **Summary of immune response**

466 The upregulated immune response genes in both organisms included innate and adaptive
 467 immunity components. An interesting phenomenon observed in the mouse (but not
 468 zebrafish) was that four genes (*C7*, *Tcra/Tcrd*, *Fcgr1a*, and *Defb30*) reached maximum
 469 transcript abundance at two different postmortem times (i.e., 1 h and 12 h) while others
 470 reached only one maximum. The variability in the gene transcript profiles suggests their
 471 regulation is effected by feedback loops.

472 **Inflammation response**

473 We would anticipate the upregulation of inflammation genes in organismal death because
 474 inflammation is an innate immunity response to injury. In the zebrafish, upregulated
 475 inflammation genes included: *Egr1*, *Egr2*, *Il1b*, Tumor necrosis factor receptor
 476 (*Tnfrsf19*), Heme oxygenase 1 (*Hmox1*), Tumor necrosis factor (*Tnf*), G-protein receptor
 477 (*Gpr31*), Interleukin-8 (*Il8*), Tumor necrosis factor alpha (*Tnfa*), Nuclear factor (NF)
 478 kappa B (*Nfkb1aa*), MAP kinase-interacting serine/threonine kinase 2b (*Mknk2b*), and
 479 Corticotropin-releasing factor receptor 1 (*Crhr1*) (Fig 5). The *Egr1* and *Egr2* genes
 480 encode transcription factors that are pro- and anti- inflammatory, respectively [47,48,76].
 481 The *Il1b* gene encodes a pro-inflammatory cytokine that plays a key role in sterile
 482 inflammation [77,78]. The *Tnfrsf19* gene encodes a receptor that has pro-inflammatory
 483 functions [79]. The *Hmox1* gene encodes an enzyme that has anti-inflammatory
 484 functions and is involved in Heme catabolism [80,81]. The *Tnf* and *Tnfa* genes encode
 485 pro-inflammatory proteins. The *Gpr31* gene encodes a pro-inflammatory protein that
 486 activates the NF- κ B signaling pathway [82]. The *Il8* gene encodes a cytokine that has
 487 pro-inflammatory properties [83]. The *Nfkb1aa* gene encodes a protein that integrates
 488 multiple inflammatory signaling pathways including *Tnf* genes [84]. The *Mknk2b* gene
 489 encodes a protein kinase that directs cellular responses and is pro-inflammatory [85].
 490 The *Crhr1* gene modulates anti-inflammatory responses [86].

491



492

493 **Fig 5. Upregulated inflammation genes by postmortem time (h). A. zebrafish; B,**
494 **mouse. Inflammation, Pro-, + ; Anti, - . Green, intermediate value; Red, maximum**
495 **value. The *Il1b* and *Mknk2b* genes were represented by two different probes.**

496

497 The upregulation of pro-inflammatory *Egr1* gene at 0.1 h was followed by the
498 upregulation of anti-inflammatory *Egr2* gene at 0.2 h, suggesting the transcription of one
499 gene is affecting the regulation of another (Fig 5). Similarly, the upregulation of the pro-
500 inflammatory *Il1b* gene at 4 h postmortem was followed by: upregulation of pro-
501 inflammatory *Tnfrsf19*, *Tnf*, *Gpr31* and *Il8* genes and anti-inflammatory *Hmox1* gene at 9
502 h, the upregulation of pro-inflammatory *Tnfa*, *Nfkb1aa*, and *Mknk2b* genes at 12 h, and
503 the upregulation of anti-inflammatory *Crhr1* gene at 24 h. Of note, while none of the
504 pro-inflammatory genes were upregulated past 48 h, the anti-inflammatory *Crhr1* gene
505 remained upregulated at 48 h. It should also be noted that the *Il1b*, *Il8*, and *Tnfa* genes
506 have been reported to be upregulated in traumatic impact injuries in postmortem tissues
507 from human brains [87].

508 In the mouse, upregulated inflammation genes included: mitogen-activated protein kinase
509 (*Map3k2*), TNF receptors (*Tnfrsf9*, *Tnfrsf14*), B-cell lymphoma 6 protein (*Bcl6*), C-C
510 chemokine receptor type 4 (*Ccr4*), Prokineticin-2 (*Prok2*), and platelet-activating factor
511 receptor (*Pafr*) (Fig 5). The *Map3k2* gene encodes a kinase that activates pro-
512 inflammatory NF- κ B genes [85]. The *Tnfrsf9* and *Tnfrsf14* genes encode receptor
513 proteins that have pro-inflammatory functions [79]. The *Bcl6* gene encodes a
514 transcription factor that has anti-inflammatory functions [88]. The *Ccr4* gene encodes a
515 cytokine receptor protein associated with inflammation [70]. The *Prok2* gene encodes a
516 cytokine-like molecule, while the *Pafr* gene encodes a lipid mediator; both have pro-
517 inflammatory functions [89,90].

518 Most inflammation-associated genes were upregulated within 1 h postmortem and
519 continued to be upregulated for 12 to 48 h. The anti-inflammatory *Bcl6* gene was
520 upregulated at two different times: 0.5 to 6 h and at 24 h suggesting that it is presumably
521 being regulated by a feedback loop. It should also be noted that pro-inflammatory
522 *Map3k2* and *Tnfrsf14* genes were not upregulated after 24 and 12 h, respectively, which
523 also suggests regulation by a putative feedback loop from the *Bcl6* gene product.

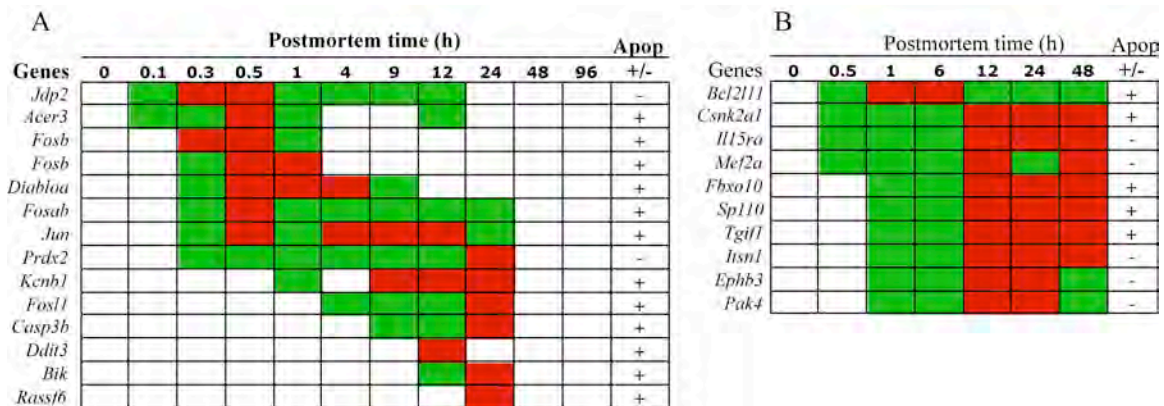
524 ***Summary of inflammation response***

525 In both organisms, some of the upregulated genes have pro-inflammatory functions while
526 others have anti-inflammatory functions, presumably reflecting regulation by feedback
527 loops. The putative feedback loops involve an initial inflammatory reaction followed by
528 an anti-inflammatory reaction to repress it [91]. The variation in the upregulation of
529 these inflammatory genes suggests an underlying regulatory network is involved in
530 organismal death.

531 **Apoptosis and related genes**

532 Since apoptotic processes kill damaged cells for the benefit of the organism as a whole,
533 we anticipated the upregulation of apoptosis genes in organismal death.

534 In the zebrafish, upregulated apoptosis genes included: Jun (*Jdp2*, *Jun*), Alkaline
 535 ceramidase 3 (*Acer3*), *Fos* (*Fosb*, *Fosab*, *Fosl1*), IAP-binding mitochondrial protein A
 536 (*Diabloa*), Peroxiredoxin-2 (*Prdx2*), Potassium voltage-gated channel member 1
 537 (*Kcnb1*), Caspase apoptosis-related cysteine peptidase 3b (*Casp3b*), DNA-damage-
 538 inducible transcript 3 (*Ddit3*), BCL2 (B-cell lymphomas 2)-interacting killer (*Bik*), and
 539 Ras association domain family 6 (*Rassf6*) (Fig 6). The *Jdp2* gene encodes a protein that
 540 represses the activity of the transcription factor activator protein 1 (*AP-1*) [92]. The
 541 *Acer3* gene encodes an enzyme that maintains cell membrane integrity/function and
 542 promotes apoptosis [93]. The *Fos* genes encode proteins that dimerize with *Jun* proteins
 543 to form part of the *AP-1* that promotes apoptosis [94,95]. The *Diabloa* gene encodes a
 544 protein that neutralizes inhibitors of apoptosis (IAP)-binding protein [95] and activates
 545 caspases [96]. The *Prdx2* gene encodes antioxidant enzymes that control cytokine-
 546 induced peroxide levels and inhibit apoptosis [97]. Although the *Kcnb1* gene encodes a
 547 protein used to make ion channels, the accumulation of these proteins in the membrane
 548 promotes apoptosis via cell signaling pathway [98]. The *Casp3b* encodes a protein that
 549 plays a role in the execution phase of apoptosis [99]. The *Ddit3* gene encodes a
 550 transcription factor that promotes apoptosis. The *Bik* gene encodes a protein that
 551 promotes apoptosis [100]. The *Rassf6* gene encodes a protein that promotes apoptosis
 552 [101].



554 **Fig 6. Upregulated apoptosis genes by postmortem time (h). A, zebrafish; B, mouse.**
 555 **Apoptosis, Pro, + ; Anti, - . Green, intermediate value; Red, maximum value. The**
 556 ***Fosb* gene was represented by two different probes.**

557

558 In the zebrafish, both anti-apoptosis *Jdp2* and pro-apoptosis *Acer3* genes were
 559 upregulated within 0.1 h postmortem (Fig 6). The upregulation of these genes was
 560 followed by the upregulation of five pro-apoptosis genes and one anti-apoptosis gene
 561 within 0.3 to 0.5 h. The transcriptional dynamics varied among the genes. Specifically,
 562 (i) the *Fosb* transcript was at low abundance after 1 h, (ii) the *Diabloa* and *Fosab*
 563 transcripts reached abundance maxima at 0.5 to 4 h and then were at low abundance after
 564 9 h for the *Diabloa* and after 24 h for the *Fosab*, (iii) the *Jun* transcript reached two
 565 maxima (one at 0.5 and another at 4 to 12 h) – and after 24 h was at low abundance, (iv)
 566 the *Prdx2* transcript showed a continuous increase in abundance, reaching a maximum at
 567 24 h and then was at low abundance. The remaining genes were pro-apoptosis and
 568 upregulated after 1 to 24 h postmortem. The *Ddit3* and *Rassf6* genes were very different

569 from the other genes in that they were upregulated at one sampling time (12 h and 24 h,
570 respectively) and then the transcripts were at low abundance. Apparently the apoptosis
571 transcripts were at low abundance after 24 h in contrast to the transcripts in other
572 categories (e.g. stress and immunity genes were upregulated for 96 h postmortem).

573 In the mouse, upregulated apoptosis-associated genes included: BCL2-like protein 11
574 (*Bcl2L11*), Casein kinase IIa (*Csnk2a1*), Interleukin 15 receptor subunit a (*Il15ra*),
575 Myocyte enhancer factor 2 (*Mef2a*), F-box only protein 10 (*Fbxo10*), Sp110 nuclear body
576 protein (*Sp110*), TGFB-induced factor homeobox 1 (*Tgif1*), Intersectin 1 (*Itsn1*) gene,
577 the Ephrin type-B receptor 3 (*Ephb3*), and the p21 protein-activated kinase 4 (*Pak4*) (Fig
578 6). The *Bcl2L11* gene encodes a protein that promotes apoptosis [102]. The *Csnk2a1*
579 gene encodes an enzyme that phosphorylates substrates and promotes apoptosis [103].
580 The *Il15ra* gene encodes an anti-apoptotic protein [104]. The *Mef2a* gene encodes a
581 transcription factor that prevents apoptosis [105]. The *Fbxo10* gene encodes a protein
582 that promotes apoptosis [106]. The *Sp110* gene encodes a regulator protein that promotes
583 apoptosis [107]. The *Tgif1* gene encodes a transcription factor that blocks signals of the
584 transforming growth factor beta (*TGFβ*) pathway; and therefore, is pro-apoptosis [108].
585 The *Itsn1* gene encodes an adaptor protein that is anti-apoptosis [109]. The *Ephb3* gene
586 encodes a protein that binds ligands on adjacent cells for cell signaling and suppresses
587 apoptosis [104]. The *Pak4* gene encodes a protein that delays the onset of apoptosis
588 [110].

589 In the mouse, pro- and anti-apoptosis genes were upregulated within 0.5 h postmortem –
590 however, with exception to *Bcl2L11*, most reached transcript abundance maxima at 12 to
591 48 h postmortem (Fig 6). The *Bcl2L11* transcripts reached abundance maxima at 1 and 6
592 h postmortem.

593 **Summary of apoptotic response**

594 In both organisms, pro- and anti-apoptosis genes were upregulated in organismal death.
595 However, the timings of the upregulation, the transcript abundance maximum, and the
596 duration of the upregulation varied by organism. The results suggest the apoptotic genes
597 and their regulation are distinctly different in the zebrafish and the mouse, with the
598 mouse genes being upregulated up to 48 h postmortem, while zebrafish genes are
599 upregulated for 24 h. Nonetheless, the pro- and anti-apoptosis genes appear to be inter-
600 regulating each another.

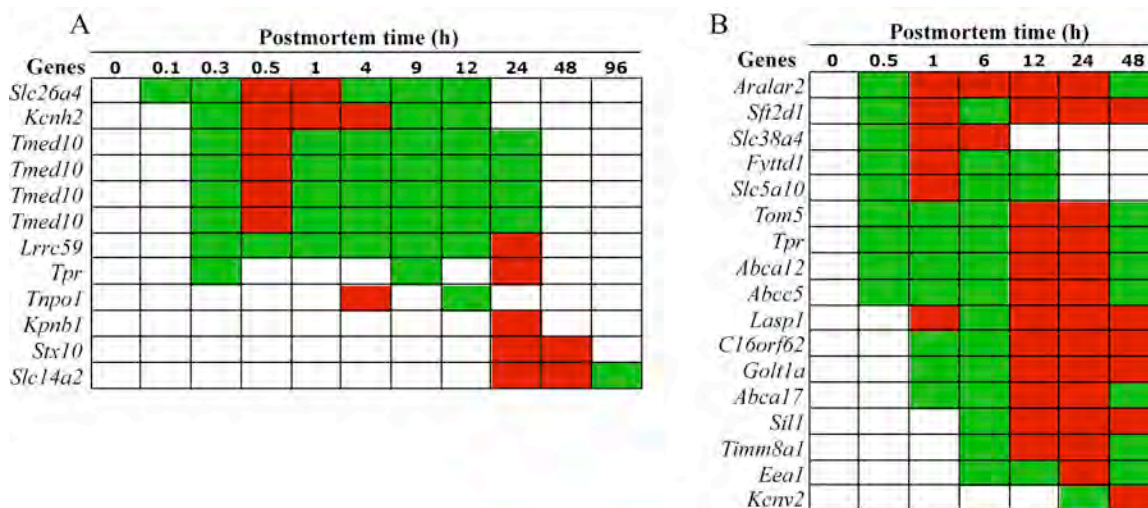
601 **Transport gene response**

602 Transport processes maintain ion/solute/protein homeostasis and are involved in
603 influx/efflux of carbohydrates, proteins, signaling molecules, and nucleic acids across
604 membranes. We anticipated that transport genes should be upregulated in organismal
605 death in response to dysbiosis.

606 In the zebrafish, upregulated transport-associated genes included: Solute carrier family 26
607 Anion Exchanger Member 4 (*Slc26a4*), Potassium channel voltage gated subfamily H
608 (*Kcnh2*), Transmembrane Emp24 domain containing protein 10 (*Tmed10*), Leucine rich
609 repeat containing 59 (*Lrrc59*), the Nucleoprotein TPR (*Tpr*), Importin subunit beta-1
610 (*Kpnb1*), Transportin 1 (*Tnpo1*), Syntaxin 10 (*Stx10*) and Urea transporter 2 (*Slc14a2*)
611 (Fig 7). Of note, the four *Tmed10* transcripts shown in Fig 7, each represents a profile

612 targeted by an independent probe. The transcription profiles of this gene were identical,
 613 indicating the high reproducibility of the Gene Meter approach. The *Slc26a4* gene
 614 encodes predrin that transports negatively-charged ions (i.e., Cl⁻, bicarbonate) across
 615 cellular membranes [111]. The *Kcnh2* gene encodes a protein used to make potassium
 616 channels and is involved in signaling [112]. The *Tmed10* gene encodes a membrane
 617 protein involved in vesicular protein trafficking [113]. The *Lrrc59*, *Tpr*, *Tnpol*, and
 618 *Kpnb1* genes encode proteins involved in trafficking across nuclear pores
 619 [114,115,116,117]. The *Stx10* gene encodes a protein that facilitates vesicle fusion and
 620 intracellular trafficking of proteins to other cellular components [118]. The *Slc14a2* gene
 621 encodes a protein that transports urea out of the cell [119].

622



623

624 **Fig 7. Upregulated transport genes by postmortem time (h) and stress category. A.**
 625 **zebrafish; B, mouse. Green, intermediate value; Red, maximum value. The *Tmed10***
 626 **gene was represented by four different probes.**

627

628 The *Slc26a4*, *Kcnh2*, *Lrrc59* and *Tpr* genes were initially upregulated within 0.3 h
 629 postmortem and continue to be expressed for 12 to 24 h. The *Tnpol* gene was
 630 upregulated at two times: 4 h and 12 h suggesting putative regulation by a feedback loop.
 631 The remaining genes were upregulated at 24 h. The upregulation of the *Slc14a2* gene
 632 suggests a build up of urea in zebrafish cells at 24 to 96 h postmortem, which could be
 633 due to the accumulation of urea under hypoxic conditions by the *Arg2* gene (see *Hsp*
 634 stress response section).

635 In the mouse, the following transport-associated genes were upregulated: Calcium-bind
 636 mitochondrial carrier protein (*Aralar2*), Sodium-coupled neutral amino acid transporter 4
 637 (*Slc38a4*), SFT2 domain containing 1 (*Sft2d1*), Uap56-interacting factor (*Fytd1*), Solute
 638 carrier family 5 (sodium/glucose co-transporter) member 10 (*Slc5a10*), Mitochondrial
 639 import receptor subunit (*Tom5*), ‘Translocated promoter region’ (*Tpr*), ATP-binding
 640 cassette transporter 12 (*Abca12*), Multidrug resistant protein 5 (*Abcc5*), LIM and SH3
 641 domain-containing protein (*Lasp1*), Chromosome 16 open reading frame 62 (*C16orf62*),
 642 Golgi transport 1 homolog A (*Golt1a*), ATP-binding cassette transporter transporter 17

643 (*Abca17*), Nucleotide exchange factor (*Sill*), Translocase of inner mitochondrial
644 membrane 8A1 (*Timm8a1*), Early endosome antigen 1 (*Eea1*), and Potassium voltage-
645 gated channel subfamily V member2 (*Kcnv2*) (Fig 7). The *Aralar2* gene encodes a
646 protein that catalyzes calcium-dependent exchange of cytoplasmic glutamate with
647 mitochondrial aspartate across the mitochondrial membrane and may function in the urea
648 cycle [120]. The *Slc38a4* gene encodes a symport that mediates transport of neutral
649 amino acids and sodium ions [121]. The *Sft2d1* gene encodes a protein involved in
650 transporting vesicles from the endocytic compartment of the Golgi complex [122]. The
651 *Fytd1* gene is responsible for mRNA export from the nucleus to the cytoplasm [123].
652 The *Slc5a10* gene encodes a protein that catalyzes carbohydrate transport across cellular
653 membranes [124]. The *Tom5* gene encodes a protein that plays a role in importation to
654 proteins destined to mitochondrial sub-compartments [125]. The *Abca12*, *Abca17* and
655 *Abc5* genes encode proteins that transport molecules across membranes [126,127,128].
656 The *Lasp1* gene encodes a protein that regulates ion-transport [129]. The *C16orf62* gene
657 encodes a protein involved in protein transport from the Golgi apparatus to the cytoplasm
658 [130]. The *Golt1a* gene encodes a vesicle transport protein [122]. The *Sill* gene encodes
659 a protein involved in protein translocation into the endoplasmic reticulum [131]. The
660 *Timm8a1* gene encodes a protein that assists importation of other proteins across inner
661 mitochondrial membranes [132]. The *Eea1* gene encodes a protein that acts as a
662 tethering molecule for vesicular transport from the plasma membrane to the early
663 endosomes [133]. The *Kcnv2* gene encodes a membrane protein involved in generating
664 action potentials [134].

665 Within 0.5 h postmortem, genes involved in: (i) ion and urea regulation (*Aralar*), (ii)
666 amino acid (*Slc38a4*), carbohydrate (*Slc5a10*), and protein (*Sft2d1*, *Tom5*) transport, (iii)
667 mRNA nuclear export (*Fytd1*, *Tpr*), and (iv) molecular efflux (*Abca12*, *Abc5*) were
668 upregulated in the mouse. The transcription profiles of these genes varied in terms of
669 transcript abundance maxima and duration of the upregulation. While the transcripts of
670 *Aralar*, *Sft2d1*, *Slc38a4*, *Fytd1* and *Slc5a10* reached abundance maxima at 1 h, those of
671 *Tom5*, *Tpr*, *Abca12*, and *Abc5* reached maxima at 12 to 24 h postmortem. The duration
672 of the upregulation also varied for these genes since most were upregulated for 48 h
673 postmortem, while the *Sft2d1*, *Fytd1* and *Slc5a10* were upregulated from 0.5 to 12 h or
674 more. The shorter duration of upregulation suggests prompt gene repression. The
675 transcript abundance of *Lasp1*, *C16orf62*, *Golt1a*, and *Abca17* increased at 1 h
676 postmortem and remained elevated for 48 h. The transcripts of *Sill*, *Timm8a1*, *Eea1*
677 increased in abundance at 6 h, while those of *Kcnv2* increased at 24 h postmortem and
678 remained elevated for 48 h.

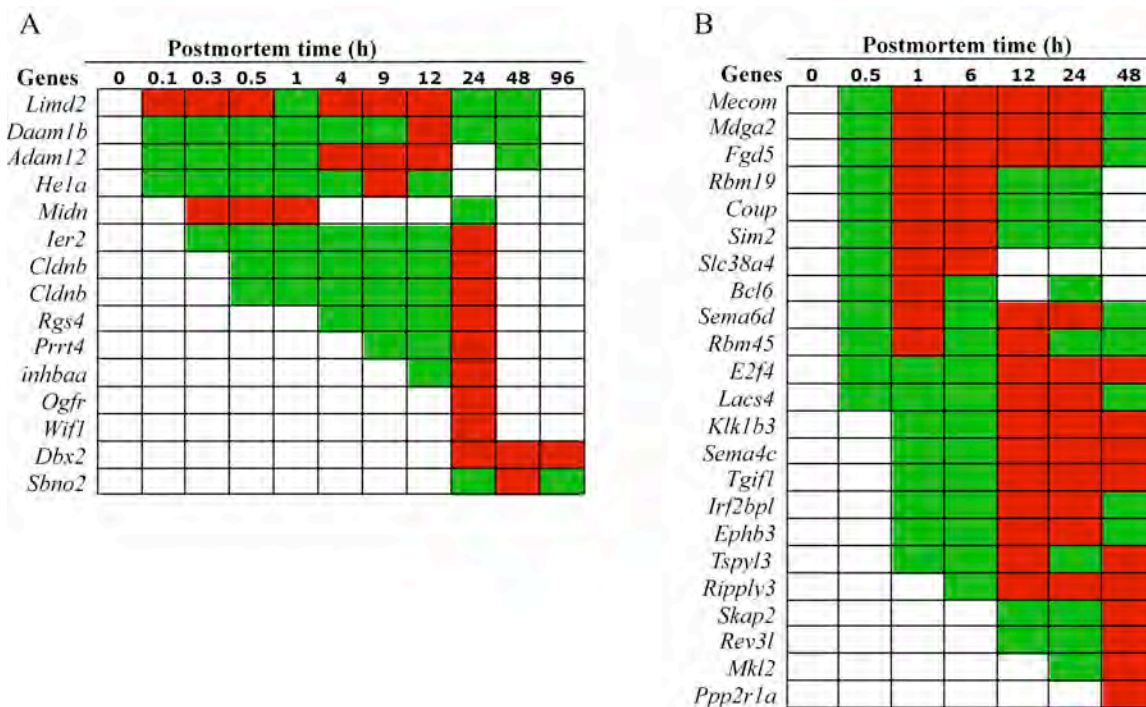
679 **Summary of transport genes**

680 The upregulation of transport genes suggests attempts by zebrafish and mice to
681 reestablish homeostasis. Although half of these genes were upregulated within 0.5 h
682 postmortem, many were upregulated at different times and for varying durations. While
683 most of the transport gene transcripts in the zebrafish were at low abundance after 24 h,
684 most transport gene transcripts in the mouse remained at high abundance at 24 to 48 h
685 postmortem.

686 **Development genes**

687 An unexpected finding in this study was the discovery of upregulated development genes
688 in organismal death. Most development genes are involved at the early stage of
689 development in the zebrafish and mouse; therefore, we did not anticipate their
690 upregulation in organismal death.

691 In the zebrafish, upregulated development genes included: LIM domain containing
692 protein 2 (*Limd2*), Disheveled-associated activator of morphogenesis 1 (*Daam1b*),
693 Meltrin alpha (*Adam12*), Hatching enzyme 1a (*He1a*), Midnolin (*Midn*), Immediate early
694 response 2 (*Ier2*), Claudin b (*Cldnb*), Regulator of G-protein signaling 4-like (*Rgs4*),
695 Proline-rich transmembrane protein 4 (*Prrt4*), Inhibin (*Inhbaa*), Wnt inhibitory factor 1
696 precursor (*Wif1*), Opioid growth factor receptor (*Ogfr*), Strawberry notch homolog 2
697 (*Sbno2*), and Developing brain homeobox 2 (*Dbx2*) (Fig 8). The *Limd2* gene encodes a
698 binding protein that plays a role in zebrafish embryogenesis [135]. The *Daam1b* gene
699 regulates endocytosis during notochord development [136]. The *Adam12* gene encodes a
700 metalloprotease-disintegrin involved in myogenesis [137]. The *He1a* gene encodes a
701 protein involved in egg envelope digestion [138]. The *Midn* gene encodes a nucleolar
702 protein expressed in the brain and is involved in the regulation of neurogenesis [139,140].
703 The *Ier2* gene encodes a protein involved in left-right asymmetry patterning in the
704 zebrafish embryos [141]. The *Cldnb* gene encodes a tight junction protein in larval
705 zebrafish [142]. The *Rgs4* gene encodes a protein involved in brain development [143].
706 The *Prrt4* gene encodes a protein that is predominantly expressed in the brain and spinal
707 cord in embryonic and postnatal stages of development. The *Inhbaa* gene encodes a
708 protein that plays a role in oocyte maturation [144]. The *Wif1* gene encodes a WNT
709 inhibitory factor that controls embryonic development [145]. The *Ogfr* gene plays a role
710 in embryonic development [146]. The *Sbno2* gene plays a role in zebrafish
711 embryogenesis [147]. The *Dbx2* gene encodes a transcription factor that plays a role in
712 spinal cord development [148].



713

714 **Fig 8. Upregulated development genes by postmortem time (h) and stress category.**
 715 **A. zebrafish; B, mouse. Green, intermediate value; Red, maximum value. The**
 716 ***Cldnb* gene was represented by two different probes.**

717

718 Although the abundances of *Limd2*, *Daam1*, *Adam12*, and *He1a* transcripts increased in
 719 the zebrafish within 0.1 h postmortem, other gene transcripts in this category increased
 720 from 0.3 to 24 h postmortem reaching abundance maxima at 24 h or more.

721 In the mouse, development genes were upregulated included: MDS1 and EVI1 complex
 722 locus protein EVI1 (*Mecom*), MAM domain containing glycosylphosphatidylinositol
 723 anchor 2 (*Mdga2*), FYVE, RhoGEF and PH domain containing 5 (*Fgd5*), RNA binding
 724 motif protein 19 (*Rbm19*), Chicken ovalbumin upstream promoter (*Coup*), Single minded
 725 homolog 2 (*Sim2*), Solute carrier family 38, member 4 (*Slc38a4*), B-cell lymphoma 6
 726 protein (*Bcl6*), Sema domain transmembrane domain (TM) cytoplasmic domain
 727 (semaphorin) 6D (*Sema6d*), RNA binding motif protein 45(*Rbm45*), Transcription factor
 728 E2F4 (*E2f4*), Long chain fatty acid- CoA Ligase 4 (*Lacs4*), Kallikrein 1-related peptidase
 729 b3 (*Klk1b3*), Sema domain, Immunoglobulin domain, transmembrane domain and short
 730 cytoplasmic domain (*Sema4c*), TGFB-induced factor homeobox 1 (*Tgif1*), Interferon
 731 regulatory factor 2-binding protein-like (*Irf2bpl*), Ephrin type-B receptor 3 (*Ephb3*),
 732 Testis-specific Y-encoded-like protein 3 (*Tspyl3*), Protein ripply 3(*Ripply3*), Src kinase-
 733 associated phosphoprotein 2 (Skap2), DNA polymerase zeta catalytic subunit (*Rev3l*),
 734 MKL/Myocardin-Like 2 (*Mkl2*), and Protein phosphatase 2 regulatory subunit A
 735 (*Ppp2r1a*) (Fig 8). The *Mecom* gene plays a role in embryogenesis and development
 736 [149]. The *Mdga2* gene encodes immunoglobins involved in neural development [150].
 737 The *Fgd5* gene is needed for embryonic development since it interacts with
 738 hematopoietic stem cells [151]. The *Rbm19* gene is essential for preimplantation
 739 development [152]. The *Coup* gene encodes a transcription factor that regulates

740 development of the eye [153] and other tissues [154]. The *Sim2* gene encodes a
741 transcription factor that regulates cell fate during midline development [155]. The
742 *Slc38a4* gene encodes a regulator of protein synthesis during liver development and plays
743 a crucial role in fetal growth and development [156,157]. The *Bcl6* gene encodes a
744 transcription factor that controls neurogenesis [158]. The *Sema6d* gene encodes a protein
745 involved in retinal development [159]. The *Rbm45* gene encodes a protein that has
746 preferential binding to poly(C) RNA and is expressed during brain development [160].
747 The *E2f4* gene is involved in maturation of cells in tissues [161]. The *Lacs4* gene plays a
748 role in patterning in embryos [162]. The *Klk1b3* gene encodes a protein that plays a role
749 in developing embryos [163]. The *Sema4c* gene encodes a protein that has diverse
750 functions in neuronal development and heart morphogenesis [164, 165]. The *Tgif1* gene
751 encodes a transcription factor that plays a role in trophoblast differentiation [166]. The
752 *Irf2bpl* gene encodes a transcriptional regulator that plays a role in female
753 neuroendocrine reproduction [167]. The *Ephb3* gene encodes a kinase that plays a role in
754 neural development [168]. The *Tspyl3* gene plays a role in testis development [169].
755 The *Ripply3* gene encodes a transcription factor involved in development of the ectoderm
756 [170]. The *Skap2* gene encodes a protein involved in actin reorganization in lens
757 development [171]. The *Rev3l* gene encodes a polymerase that can replicate past certain
758 types of DNA lesions and is necessary for embryonic development [172]. The *Mkl2* gene
759 encodes a transcriptional co-activator is involved in the formation of muscular tissue
760 during embryonic development [173]. The *Ppp2r1a* gene plays a role in embryonic
761 epidermal development [174].

762 While the *Mecom*, *Mdga2*, *Fgd5*, *Rbm19*, *Coup*, *Sim2*, *Slc38a4*, *Bcl6*, *Sema6d*, *Rbm45*,
763 *E2f4* and *Lacs4* genes were upregulated within 0.5 h postmortem, the other genes were
764 upregulated at 1 h to 48 h with most transcripts reaching abundance maxima at 12 h or
765 more.

766 **Summary of development genes**

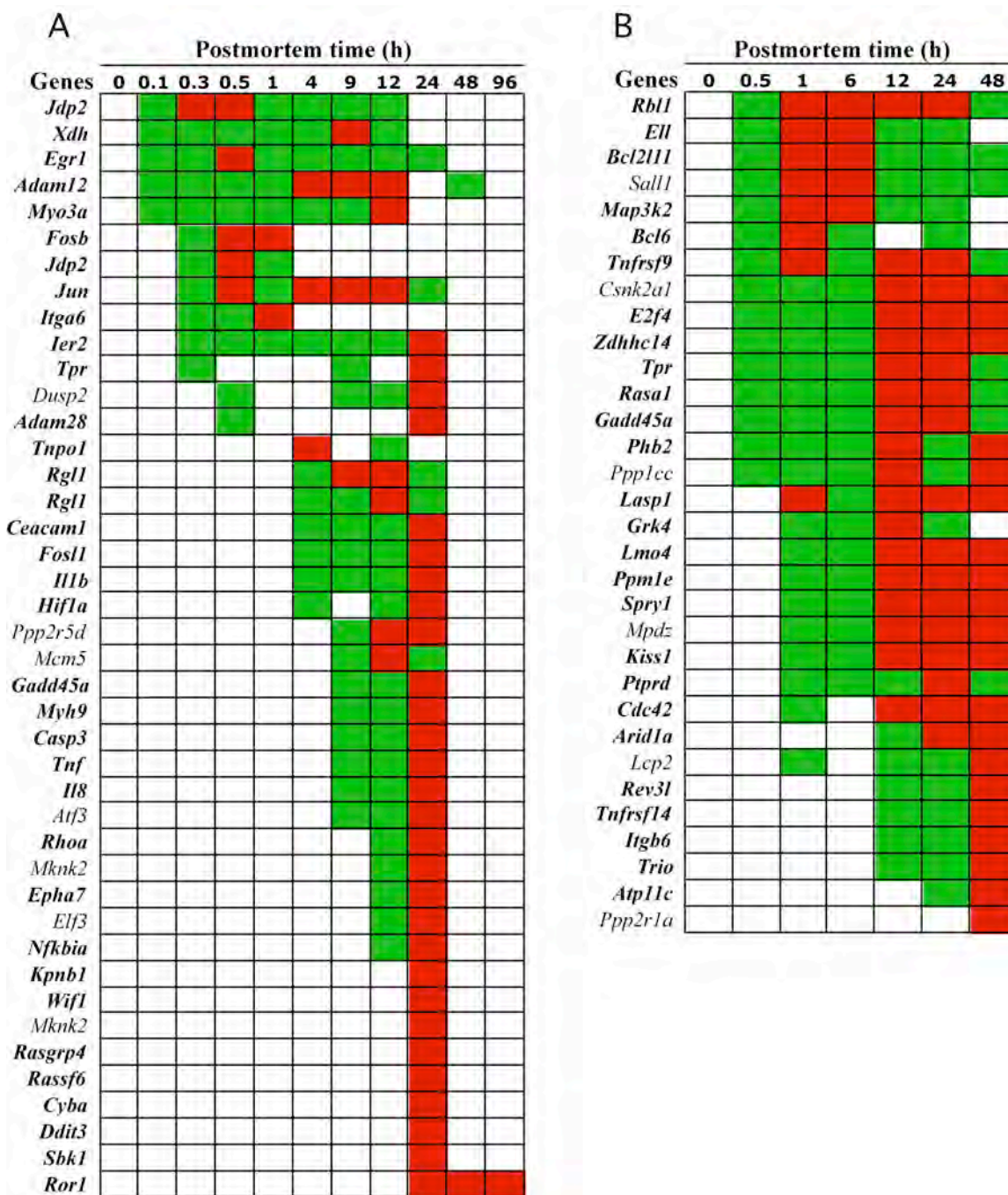
767 In organismal death, there is progressive activation of developmental genes suggesting
768 that they are no longer silenced. A possible reason for this activation is that postmortem
769 physiological conditions resemble those during development.

770 **Cancer genes**

771 There are a number of databases devoted to cancer and cancer-related. Upon cross-
772 referencing the genes found in this study, we discovered a significant overlap. The genes
773 found in this search are presented below.

774 In the zebrafish, the following cancer genes were upregulated: *Jdp2*, xanthine
775 dehydrogenase (*Xdh*), *Egr1*, *Adam12*, myosin-IIIa (*Myo3a*), *Fosb*, *Jun*, Integrin alpha 6b
776 (*Itga6*), *Ier2*, *Tpr*, Dual specificity protein phosphatase 2 (*Dusp2*), Disintegrin and
777 metalloproteinase domain 28 (*Adam28*), *Tnpo1*, Ral guanine nucleotide dissociation
778 stimulator-like (*Rgl1*), Carcinoembryonic antigen-related cell adhesion molecule 5
779 (*Ceacam1*), *Fosl1*, *Il1b*, *Hif1a*, Serine/threonine-protein phosphatase 2A regulatory
780 (*Ppp2r5d*), DNA replication licensing factor (*Mcm5*), *Gadd45*, Myosin-9 (*Myh9*), *Casp3*,
781 *Tnf*, *Il8*, Cyclic AMP-dependent transcription factor (*Atf3*), small GTPase (*RhoA*),
782 *Mknk2*, Ephrin type-A receptor 7 precursor (*Epha7*), ETS-related transcription factor
783 (*Elf3*), *Nfkb1a*, *Kpnb1*, *Wif1*, RAS guanyl-releasing protein 1 (*Rasgrp*), Ras association

784 domain-containing protein 6 (*Rassf6*), *Cyba*, DNA-damage-inducible transcript 3 (*Ddit3*),
 785 Serine/threonine-protein kinase (*Sbk1*), and Tyrosine-protein kinase transmembrane
 786 receptor (*Ror1*) (Fig 9).



787

788 **Fig 9. Upregulated cancer genes by postmortem time (h). A, Zebrafish; B, Mouse.**
 789 **Green, intermediate value; Red, maximum value. Bold gene name means it was**
 790 **found in more than one cancer database. The *Rgl1* gene was represented by two**
 791 **different probes.**

792

793 In the mouse, the following cancer genes were upregulated: retinoblastoma-like protein 1
794 (*Rbl1*), Elongation factor RNA polymerase II (*Ell*), Bcl-2-like protein 11 (*Bcl2l11*), Sal-
795 like protein 1 (*Sall1*), *Map3k2*, *Bcl6*, *Tnfrsf9*, CK2 target protein 2 (*Csnk2a1*),
796 Transcription factor E2f4 (*E2f4*), Zinc finger DHHC-type containing 14 (*Zdhhc14*), *Tpr*,
797 RAS p21 protein activator 1 (*Rasa1*), *Gadd45*, prohibitin (*Phb2*), Serine/threonine-
798 protein phosphatase PP1-gamma catalytic (*Ppp1cc*), *Lasp1*, G protein-coupled receptor
799 kinase 4 (*Grk4*), LIM domain transcription factor (*Lmo4*), Protein phosphatase 1E
800 (*Ppm1e*), Protein sprouty homolog 1 (*Spry1*), Multiple PDZ domain protein (*Mpdz*),
801 Kisspeptin receptor (*Kiss1*), Receptor-type tyrosine-protein phosphatase delta precursor
802 (*Ptprd*), Small effector protein 2-like (*Cdc42*), AT-rich interactive domain-containing
803 protein 1A (*Arid1a*), Lymphocyte cytosolic protein 2 (*Lcp2*), DNA polymerase zeta
804 catalytic subunit (*Rev3l*), *Tnfrsf14*, Integrin beta-6 precursor (*Itgb6*), Triple functional
805 domain protein (*Trio*), ATPase class VI type 11C (*Atp11c*), and Serine/threonine-protein
806 phosphatase 2A regulatory (*Ppp2r1a*) (Fig 9).

807 **Summary of cancer genes**

808 These genes were classified as “cancer genes” in a Cancer Gene Database [7] (Fig 9).
809 The timing, duration and peak transcript abundances differed within and between
810 organisms. Note that some transcripts had two abundance maxima. In the zebrafish, this
811 phenomenon occurred for *Adam12*, *Jun*, *Tpr*, *Dusp2*, *Tnpo1*, and *Hif1a* and in the mouse,
812 *Bcl6*, *Tnfrsf9*, *Lasp1*, *Cdc42*, and *Lcp2*, and is consistent with the notion that the genes are
813 being regulated through feedback loops.

814 **Epigenetic regulatory genes**

815 Epigenetic regulation of gene expression involves DNA methylation and histone
816 modifications of chromatin into active and silenced states [175]. These modifications
817 alter the condensation of the chromatin and affect the accessibility of the DNA to the
818 transcriptional machinery. Although epigenetic regulation plays important role in
819 development, modifications can arise stochastically with age or in response to
820 environmental stimuli [176]. Hence, we anticipated that epigenetic regulatory genes
821 should be involved in organismal death.

822 In the zebrafish, the following epigenetic genes were upregulated: Jun dimerization
823 protein 2 (*Jdp2*), Chromatin helicase protein 3 (*Chd3*), Glutamate-rich WD repeat-
824 containing protein 1 (*Grwd1*), Histone H1 (*Histh1l*), Histone cluster 1, H4-like
825 (*Hist1h46l3*) and Chromobox homolog 7a (*Cbx7a*) (Fig 10). The *Jdp2* gene is thought to
826 inhibit the acetylation of histones and repress expression of the c-Jun gene [177]. The
827 *Chd3* gene encodes a component of a histone deacetylase complex that participates in the
828 remodeling of chromatin [178]. The *Grwd1* gene is thought to be a histone-binding
829 protein that regulates chromatin dynamics at the replication origin [179]. The *Histh1l*
830 gene encodes a histone protein that binds the nucleosome at the entry and exit sites of the
831 DNA and the *Hist1h46l3* gene encodes a histone protein that is part of the nucleosome
832 core [180]. The *Cbx7a* gene encodes an epigenetic regulator protein that binds non-
833 coding RNA and histones and represses gene expression of a tumor suppressor [181].

834

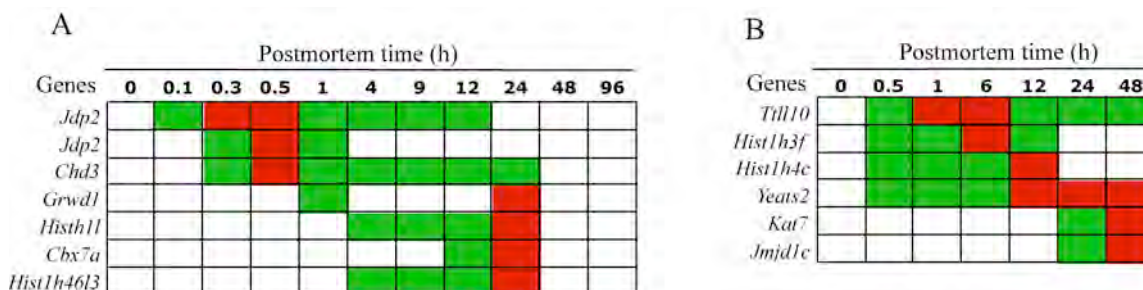


Fig 10. Upregulated epigenetic genes by postmortem time (h). A, Zebrafish; B, Mouse. Green, intermediate value; Red, maximum value. Bold gene name means it was found in more than one cancer database. The *Jdp2* gene was represented by two different probes.

840

841 Both *Jdp2* and *Chd3* genes were upregulated within 0.3 h postmortem, with their
 842 transcripts reaching abundance maxima at 0.5 h. Note that two different probes targeted
 843 the *Jdp2* transcript. The *Grwd1* gene was upregulated at 1 h and 24 h postmortem. The
 844 histone genes were upregulated at 4 h postmortem with their transcripts reaching
 845 abundance maxima at 24 h. The *Cbx7a* gene was upregulated at 12 h and its transcript
 846 reached an abundance maximum at 24 h. Transcripts of these genes were at low
 847 abundance after 24 h.

848 In the mouse, the following epigenetic genes were upregulated: Tubulin tyrosine ligase-
 849 like family member 10 (*Till10*), Histone cluster 1 H3f (*Hist1h3f*), Histone cluster 1 H4c
 850 (*Hist1h4c*), YEATS domain containing 2 (*Yeats2*), Histone acetyltransferase (*Kat7*), and
 851 Probable JmjC domain-containing histone demethylation protein 2C (*Jmjd1c*) (Fig 10).
 852 The *Till10* gene encodes a polyglycylase involved in modifying nucleosome assembly
 853 protein 1 that affects transcriptional activity, histone replacement, and chromatin
 854 remodeling [182]. The *Hist1h3f* and *Hist1h4c* genes encode histone proteins are the core
 855 of the nucleosomes [183]. The *Yeats2* gene encodes a protein that recognizes histone
 856 acetylations so that it can regulate gene expression in the chromatin [184]. The *Kat7*
 857 gene encodes an acetyltransferase that is a component of histone binding origin-of-
 858 replication complex, which acetylates chromatin and therefore regulates DNA replication
 859 and gene expression [185]. The *Jmjd1c* gene encodes an enzyme that specifically
 860 demethylates 'Lys-9' of histone H3 and is implicated in the reactivation of silenced genes
 861 [186].

862 The *Till10*, *Yeats2* and histone protein genes were upregulated 0.5 h postmortem but their
 863 transcripts reached abundance maxima at different times with the *Till10* transcript
 864 reaching a maximum at 1 to 6 h, the histone transcripts reaching maxima at 6 and 12 h
 865 postmortem, and the *Yeats2* transcript reaching maxima at 12 to 24 h postmortem (Fig
 866 10). The *Kat7* and *Jmjd1c* genes were upregulated at 24 h and their transcripts reached
 867 abundance maxima at 48 h postmortem.

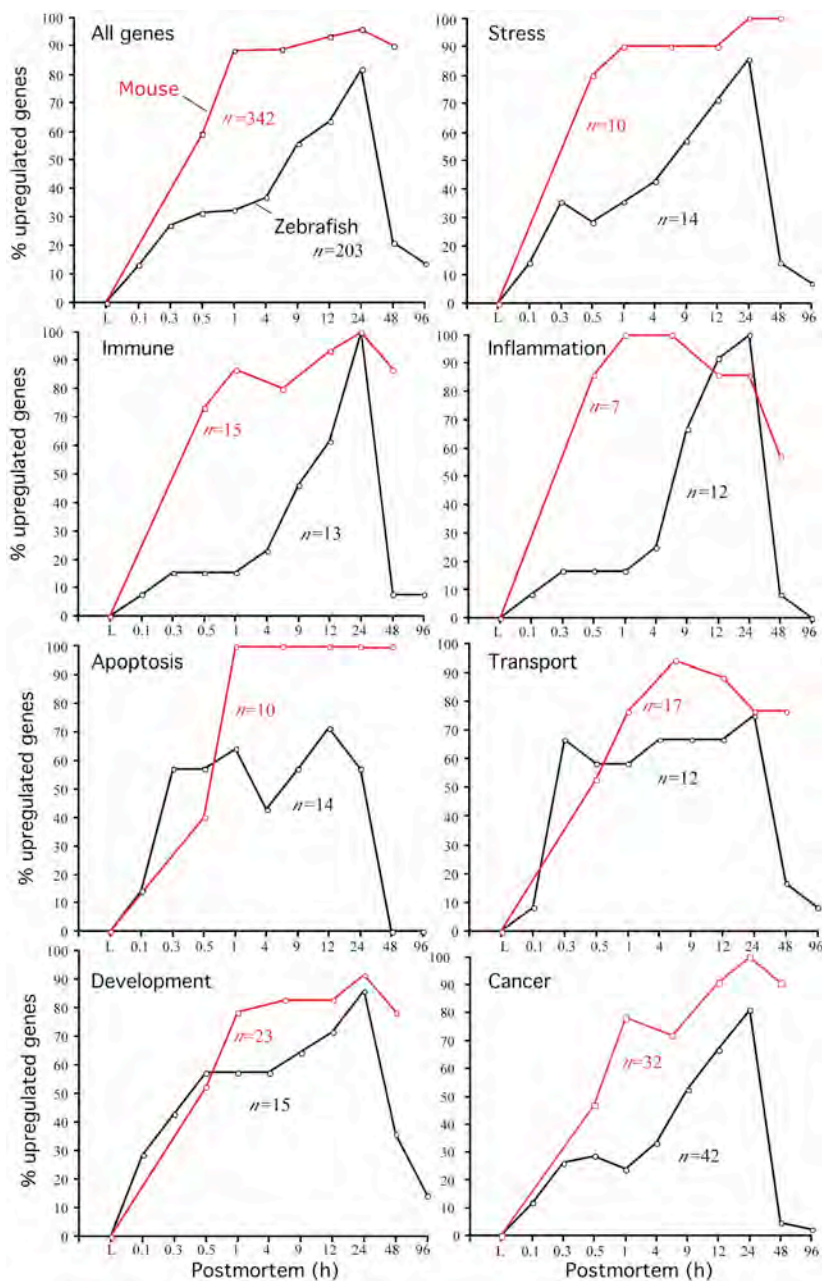
868 **Summary of epigenetic regulatory genes**

869 The upregulation of genes encoding histone proteins, histone-chromatin modifying
 870 proteins, and proteins involved in regulating DNA replication at the origin were common
 871 to the zebrafish and the mouse. These findings indicate that epigenetic regulatory genes

872 are modifying chromatin structure by regulating the accessibility of transcription factors
873 to the promoter or enhancer regions in organismal death.

874 **Percentage of upregulated genes with postmortem time**

875 The % of upregulated genes was defined as the number of upregulated genes at a specific
876 postmortem time over the total number of upregulated genes in a category. A
877 comparison of the % of upregulated genes by postmortem time of all upregulated genes
878 revealed similarities between the zebrafish and the mouse. Specifically, most genes were
879 upregulated between 0.5 to 24 h postmortem, and after 24 h, the upregulation of most
880 genes stopped (Fig 11, “All genes”). It should be noted that the same pattern was found
881 in stress, transport and development categories for both organisms. However, in the
882 zebrafish, the immunity, inflammation, apoptosis and cancer categories differed from the
883 mouse. Specifically, the genes in the immunity, inflammation, and cancer categories
884 were upregulated much later (1 to 4 h) in the zebrafish than the mouse, and the duration
885 of upregulation was much shorter. For example, while 90% of the genes in the immunity
886 and inflammation categories were upregulated in the mouse within 1 h postmortem, less
887 than 30% of the genes were upregulated in the zebrafish (Fig 11), indicating a slower
888 initial response. It should be noted that while the number of upregulated immunity genes
889 reaching transcript abundance maxima occurred at 24 h postmortem in both organisms,
890 the number of inflammation genes reaching transcript abundance maxima occurred at 1 to
891 4 h in the mouse, and 24 h in the zebrafish. The significance of these results is that the
892 inflammation response occurs rapidly and robustly in the mouse while in the zebrafish, it
893 takes longer to establish, which could be attributed to phylogenetic differences. There
894 were significant differences in the upregulation of apoptosis genes between the zebrafish
895 and the mouse. In the mouse, the number of upregulated apoptosis genes reached 100%
896 at 1 h postmortem and remained sustained for 48 h postmortem while the % of
897 upregulated genes in the zebrafish never reached 70% and gene upregulation was
898 abruptly stopped after 12 h.



899

900 **Fig 11. % of upregulated genes by postmortem time and category. Number of total**
901 **genes by organism and category are shown. “All genes” refers to the genes that**
902 **significantly contributed to the ordination plots. Mouse is red; Zebrafish is black.**

903

904 **DISCUSSION**

905 **Active gene expression or residual transcription levels?**

906 One could argue that our study identifies only residual transcription levels of pre-
907 synthesized mRNA (rather than newly-synthesized mRNA) in dead tissues that happen to

908 be enriched with postmortem time. In other words, the observed upregulation of genes
909 may be viewed as an artifact merely reflecting the “enrichment of specific mRNA
910 transcripts” (e.g. stable mRNA) with time. The data, however, does not support this idea
911 because if it were true, one would expect stable transcripts to monotonically increase with
912 time, as they become more enriched (higher abundances) with postmortem time. The
913 data show that the transcripts of most upregulated genes did not display monotonic
914 behavior; rather, the transcripts reached abundance maximum (peak) or maxima (peaks)
915 at various postmortem times (Fig 2D and 2E). This finding should not be a surprise
916 because a statistical procedure was implemented to detect genes that were significantly
917 upregulated – which is essentially selecting gene transcriptional profiles that had peaks.
918 The statistics for the procedure was calibrated with more than a billion simulations. The
919 simulation process corrected for multiple comparisons. The residual transcription level
920 and enrichment idea is also not supported by transcriptional profiles displaying an up-,
921 down-, and up- regulation pattern, which putatively indicates feedback loops (Fig S3).
922 Similarly, simple differential decay rates of mRNAs would not display this pattern
923 because a transcript cannot be stable at one postmortem time, unstable at a subsequent
924 time, and then stable again. A mRNA transcript is either stable or it is not. In
925 conclusion, the gene profiles showing upregulation are the results of active transcription.

926
927 It should be noted that postmortem upregulation of genes has been previously reported in
928 cadavers. Using reverse transcription real-time quantitative PCR (RT-RTqPCR), a study
929 showed significant increases in expression of myosin light chain 3 (*Myl3*), matrix
930 metalloprotease 9 (*Mmp9*), and vascular endothelial growth factor A (*Vegfa*) genes in
931 body fluids after 12 h postmortem (187). Interestingly, postmortem upregulation of
932 myosin-related and matrix metalloprotease genes was also found in our study.
933 Specifically, the myosin-related genes included: Myosin-Ig (*Myo1g*) in the mouse, and
934 Myosin-IIIa (*Myo3a*) and Myosin-9 (*Myh9*) in the zebrafish. The matrix
935 metalloproteinase gene included the metalloproteinase-14 (*Mmp14b*) gene in the
936 zebrafish. The *Myo1g* gene encodes a protein regulating immune response (189), the
937 Myosin-IIIa (*Myo3a*) gene encodes an uncharacterized protein, the Myosin-9 (*Myh9*)
938 gene encodes a protein involved in embryonic development (190), and the *Mmp14b* gene
939 encodes an enzyme regulating cell migration during zebrafish gastrulation (188). The
940 *Myo1g*, *Myh9* and *Mmp14b* transcripts increased right after death and reached abundance
941 maxima at 24 h postmortem, while the *Myo3a* transcript reached an abundance maximum
942 at 12 h postmortem. The significance of these results is two-fold: (i) two different
943 technologies (RT-RTqPCR and Gene Meters) have now demonstrated active postmortem
944 upregulation of genes and this expression has now been reported in three organisms
945 (human, zebrafish, and mouse), and (ii) there might be significant overlap in genes
946 upregulated in death as we have showed with myosin- and matrix metalloprotease genes,
947 which warrants further studies using other vertebrates. The purpose of such studies
948 would be to understand common mechanisms involved in the shutdown of highly ordered
949 biological systems.

950 **Why study gene expression in death?**

951 The primary motivation for the study was driven by curiosity in the processes of shutting
952 down a complex biological system – which has received little attention so far. While the

953 development of a complex biological system requires time and energy, its shutdown and
954 subsequent disassembly entails the dissipation of energy and unraveling of the complex
955 structures, which does not occur instantaneously and could provide insights into
956 interesting paths. Moreover, other fields of research have examined the shutdown of
957 complex systems (e.g., societies [191], government [192], electrical black outs [193]).
958 Yet, to our knowledge, no study has examined long-term postmortem gene expression of
959 vertebrates kept in their native conditions. The secondary motivation for the study was to
960 demonstrate the precision of Gene Meter technology for gene expression studies to
961 biologists who believe that high throughput DNA sequencing is the optimal approach.

962 **Thermodynamic sinks**

963 We initially thought that sudden death of a vertebrate would be analogous to a car driving
964 down a highway and running out of gas. For a short time, engine pistons will move up
965 and down and spark plugs will spark -- but eventually the car will grind to a halt and
966 “die”. Yet, in our study we find hundreds of genes are upregulated many hours
967 postmortem, with some (e.g., *Kcnv2*, *Pafr*, *Dege2*, *Ogfod1*, *Ppp2rla*, *Ror1*, and *Iftm1*)
968 upregulated days after organismal death. This finding is surprising because in our car
969 analogy, one would not expect window wipers to suddenly turn on and the horn to honk
970 several days after running out of gas.

971 Since the postmortem upregulation of genes occurred in both the zebrafish and the mouse
972 in our study, it is reasonable to suggest that other multicellular eukaryotes will display a
973 similar phenomenon. What does this phenomenon mean in the context of organismal
974 life? We conjecture that the highly ordered structure of an organism – evolved and
975 refined through natural selection and self-organizing processes – undergoes a
976 thermodynamically driven process of spontaneous disintegration through complex
977 pathways, which apparently involve the upregulation of genes and feedback loops. While
978 evolution played a role in pre-patterning of these pathways, it does not play any role in its
979 disintegration fate. One could argue that some of these pathways have evolved to favor
980 healing or “resuscitation” after severe injury. For example, the upregulation of
981 inflammation response genes indicate that a signal of infection or injury is sensed by the
982 still alive cells after death of the body. Alternatively, the upregulation may be due to fast
983 decay of some repressors of genes or whole pathways (see below). Hence, it will be of
984 interest to study this in more detail, since this could, for example, provide insights into
985 how to better preserve organs retrieved for transplantation.

986 **Chemical automator – on the way down to equilibrium**

987 As one would expect, a living system is a collection of chemical reactions linked together
988 by the chemicals participating in them. Having these reactions to depend on one another
989 to a certain extent, we conjecture that the observed upregulation of genes is due to
990 thermodynamic and kinetic controls that are encountered during organismal death. For
991 example, epigenetic regulatory genes that were upregulated included histone modification
992 genes (e.g., *Histh1l*) and genes interacting with chromatin (e.g., *Grwd1*, *Chd3*, *Yeats*,
993 *Jmjd1c*) (Fig 10). It is possible that the activation of these genes was responsible for the
994 unraveling of the nucleosomes, which enabled transcription factors and RNA
995 polymerases to transcribe developmental genes that have been previously silenced since

996 embryogenesis. The energy barrier in this example is the tightly wrapped nucleosomes
997 that previously did not allow access to developmental genes. Other energy or entropy
998 barriers could be nucleopores that allow the exchange of mRNA and other molecules
999 between the mitochondria and the cytosol (e.g., *Tpr*, *Tnp1*, *Lrrc59*), or the ion/solute
1000 protein channels (e.g., *Aralar2*, *Slc38a4*) that control intracellular ions that regulate
1001 apoptotic pathways [194,195].

1002 The upregulation of genes indicates new molecules were synthesized. Hence, there was
1003 sufficient energy and resources (e.g., RNA polymerase, dNTPs) in dead organisms to
1004 maintain gene transcription to 96 h (e.g., *Zfand4*, *Tox2*, and *Slc14a2*) in the zebrafish and
1005 to 48 h (e.g., *Deg2*, *Ogfod1*, and *Ifitm1*) in the mouse. Gene transcription was apparently
1006 not prevented due to a lack of energy or resources. Several genes exhibited apparent
1007 regulation by feedback loops in their transcriptional profiles (e.g., *Rbm45* and *Cdc42*
1008 genes in the mouse (Fig 8 and 9, respectively; Fig S3)). Hence, an underlying regulatory
1009 network appears to be still turning “on” and “off” genes in organismal death.

1010 **Interrupt the shutdown?**

1011 A living biological system is a product of natural selection and self-organizing processes
1012 [196]. Genes are transcribed and proteins translated in response to genetic and epigenetic
1013 regulatory networks that sustain life. In organismal death, we assumed most of the
1014 genetic and epigenetic regulatory networks operating in life would become disengaged
1015 from the rest of the organism. However, we found that “dead” organisms turn genes on
1016 and off in a non-random manner (Fig 2D and 2E). There is a range of times in which
1017 genes are upregulated and transcript abundances are maximized. While most genes are
1018 upregulated within 0.5 h postmortem (Fig 11), some are upregulated at 24 h and still
1019 others at 48 h. A similar pattern occurs with peak transcript abundances and the timing
1020 when upregulation is apparently stopped. These differences in timings and abundances
1021 suggest some sort of global regulation network is still operating in both organisms. What
1022 makes gene expression of life different from gene expression in death is that postmortem
1023 upregulation of genes offers no obvious benefit to an organism. We argue that self-
1024 organizing processes driven by thermodynamics are responsible for the postmortem
1025 upregulation of genes. We emphasize that such postmortem conditions could allow
1026 investigators to tease apart evolution from self-organizing processes that are typically
1027 entangled in life.

1028 Since our results show that the system has not reached equilibrium yet, it would be
1029 interesting to address the following question: *what would happen if we arrested the*
1030 *process of dying by providing nutrients and oxygen to tissues?* It might be possible for
1031 cells to revert back to life or take some interesting path to differentiating into something
1032 new or lose differentiation altogether, such as in cancer. We speculate that the recovering
1033 cells will likely depend on the postmortem time – at least when such potentially
1034 interesting effects might be seen.

1035 **Methodological validity**

1036 The Gene Meter approach is pertinent to the quality of the microarray output obtained in
1037 this study because conventional DNA microarrays yield noisy data [197,198]. The Gene
1038 Meter approach determines the behavior of every microarray probe by calibration –

1039 which is analogous to calibrating a pH meter with buffers. Without calibration, the
1040 precision and accuracy of a meter is not known, nor can one know how well the
1041 experimental data fits to the calibration (i.e., R^2). In the Gene Meter approach, the
1042 response of a probe (i.e., its behavior in a dilution series) is fitted to either Freundlich or
1043 Langmuir adsorption model, probe-specific parameters are calculated. The “noisy” or
1044 “insensitive” probes are identified and removed from further analyses. Probes that
1045 sufficiently fit the model are retained and later used to calculate the abundance of a
1046 specific gene in a biological sample. The models take into consideration the non-linearity
1047 of the microarray signal and the calibrated probes do not require normalization
1048 procedures to compare biological samples. In contrast, conventional DNA microarray
1049 approaches are biased because different normalizations can yield up to 20 to 30%
1050 differences in the up- or down-regulation depending on the procedure selected [199-202].
1051 We recognize that next-generation-sequencing (NGS) approaches could have been used
1052 to monitor gene expression in this study. However, the same problems of normalization
1053 and reproducibility (mentioned above) are pertinent to NGS technology [203]. Hence,
1054 the Gene Meter approach is currently the most advantageous to study postmortem gene
1055 expression in a high throughput manner.

1056 **Practical implications**

1057 The postmortem upregulation of genes in the mouse has relevance to transplantation
1058 research. We observed clear qualitative and quantitative differences between two organs
1059 (liver and brain) in the mouse in their degradation profiles (Fig 1). We also showed the
1060 upregulation of immunity, inflammation and cancer genes within 1 h of death (Fig 11). It
1061 would be interesting to explore if these differences are comparable to what occurs in
1062 humans, and we wonder how much of the transplant success could be attributed to
1063 differences in the synchronicity of postmortem expression profiles rather than
1064 immunosuppression agents [204,205]. Our study provides an alternative perspective to
1065 the fate of transplant recipients due to the upregulation of regulatory and response genes,
1066 after the sample has been harvested from the donor.

1067 **Conclusion**

1068 This is the first study to demonstrate active, long-term expression of genes in organismal
1069 death that raises interesting questions relative to transplantology, inflammation, cancer,
1070 evolution, and molecular biology.

1071

1072 **Competing Interests**

1073 The authors declare that they have no competing interests.

1074

1075 **Authors' contributions**

1076 DT, RN, TDL and AEP designed the study. AEP, RN, TDL carried out the molecular
1077 genetic studies. BGL and AEP determined the statistically significant upregulated genes.
1078 SS and PAN annotated the genes. AEP and PAN conducted the statistical analyses and
1079 wrote the manuscript. All authors read and approved the final manuscript.

1080 **Acknowledgements**

1081 We thank Till Sckerl for help with sacrificing the mice, Nicole Thomsen for help with
1082 tissue and RNA processing, and Elke Blohm-Sievers for microarray work. We thank
1083 Russell Bush for his helpful advice on thermodynamics and entropic barriers and M.
1084 Colby Hunter for proof-reading the manuscript.

1085

1086 **Financial disclosure** The work was supported by funds from the National Cancer
1087 Institute P20 Partnership grant (P20 CA192973 and P20 CA192976) and the Max-
1088 Planck-Society.

1089

1090

1091

1092 **REFERENCES**

- 1093 1. Monod J. Genetic regulatory mechanisms in the synthesis of proteins. *J Mol Biol.*
1094 1961;3: 318.
- 1095 2. Zong WX, Thompson CB. Necrotic death as a cell fate. *Genes Dev.* 2006, 20: 1.
- 1096 3. GalluzziL, Bravo-San Pedro JM, Kroemer G. Organelle-specific initiation of cell
1097 death. *Nat Cell Biol.* 2014;16: 728-736.
- 1098 4. Ferriferri_2001 KF, Kroemer G. Organelle-specific initiation of cell death pathways.
1099 *Nat Cell Biol.* 2001;3: E255.
- 1100 5. Syntichakisyntichaki_2002 P, Tavernarakis N. Death by necrosis. Uncontrollable
1101 catastrophe, or is there order behind the chaos? *EMBO Rep.* 2002;3: 604.
- 1102 6. Pozhitkov AE, Noble PA, Bryk J, Tautz D. A revised design for microarray
1103 experiments to account for experimental noise and uncertainty of probe response.
1104 *PLoS One.* 2014;9: e91295.
- 1105 7. Domazet-Loso T, Tautz D. Phylostratigraphic tracking of cancer genes suggests a
1106 link to the emergence of multicellularity in metazoa. *BMC Biol.* 2010;8: 66. doi:
1107 10.1186/1741-7007-8-66.
- 1108 8. Seear PJ, Sweeney GE. Stability of RNA isolated from post-mortem tissues of
1109 Atlantic salmon (*Salmo salar* L.). *Fish Physiol Biochem.* 2008;34: 19-24. doi:
1110 10.1007/s10695-007-9141-x.
- 1111 9. Bahar B, Monahan FJ, Moloney AP, Schmidt O, MacHugh DE, Sweeney T. Long-
1112 term stability of RNA in post-mortem bovine skeletal muscle, liver and subcutaneous
1113 adipose tissues. *BMC Mol Biol.* 2007;8: 108.
- 1114 10. Inoue H, Kimura A, Tuji T. Degradation profile of mRNA in a dead rat body: basic
1115 semi-quantification study. *Forensic Sci Int.* 2002;130: 127-32.
- 1116 11. Johnson SA, Morgan DG, Finch CE. Extensive postmortem stability of RNA from rat
1117 and human brain. *J Neurosci Res.* 1986;16: 267-80.
- 1118 12. Catts VS, Catts SV, Fernandez HR, Taylor JM, Coulson EJ, Lutze-Mann LH. A
1119 microarray study of post-mortem mRNA degradation in mouse brain tissue. *Brain*
1120 *Res Mol Brain Res.* 2005;138: 164-77.
- 1121 13. Heinrich M, Matt K, Lutz-Bonengel S, Schmidt U. Successful RNA extraction from
1122 various human postmortem tissues. *Int J Legal Med.* 2007;121: 136-42.
- 1123 14. Neymotin, Athanasiadou R, Gresham D. Determination of in vivo RNA kinetics
1124 using RATE-seq. *RNA.* 2014;20: 1645.
- 1125 15. Spilka R, Ernst C, Bergler H, Rainer J, Flechsig S, Vogetseder A, Lederer E, Benesch
1126 M, Brunner A, Geley S, Eger A, Bachmann F, Doppler W, Obrist P, Haybaeck J.
1127 eIF3a is over-expressed in urinary bladder cancer and influences its phenotype
1128 independent of translation initiation. *Cell Oncol (Dordr).* 2014;37: 253

- 1129 16. Bortolotti GR, Tella JL, Baos R, Marchant TA. Stress response during development
1130 predicts fitness in a wild, long lived vertebrate. *Proc Natl Acad Sci USA*. 2007;104:
1131 8880-4.
- 1132 17. Skaggs HS, Xing H, Wilkerson DC, Murphy LA, Hong Y, Mayhew CN, Sarge KD.
1133 HSF1-TPR interaction facilitates export of stress-induced HSP70 mRNA. *J Biol*
1134 *Chem*. 2007;282: 33902-7.
- 1135 18. Snow CJ, Paschal BM. Roles of the nucleoporin Tpr in cancer and aging. *Adv Exp*
1136 *Med Biol*. 2014;773: 309-22. doi: 10.1007/978-1-4899-8032-8_14.
- 1137 19. David-Watine B. Silencing nuclear pore protein Tpr elicits a senescent-like
1138 phenotype in cancer cells. *PLoS One*. 2011;6: e22423. doi:
1139 10.1371/journal.pone.0022423.
- 1140 20. Kadeba PI, Scammel JG, Cioffi DL. The chaperone heat shock protein 90 (Hsp90)
1141 participates in the endothelial store operated calcium entry heterocomplex. *FASEB J*.
1142 2013;27: 724.4
- 1143 21. Mayer MP, Bukau B. Hsp70 chaperones: cellular functions and molecular
1144 mechanism. *Cell Mol Life Sci*. 2005;62: 670-84.
- 1145 22. Jakobsson ME, Davydova E, Małecki J, Moen A, Falnes, PØ. *Saccharomyces*
1146 *cerevisiae* eukaryotic elongation factor 1A (eEF1A) is methylated at Lys-390 by a
1147 METTL21-like methyltransferase. *PLoS One* 2015;
1148 doi:10.1371/journal.pone.0131426.t002.
- 1149 23. Höhfeld J, Hartl FU. Requirement of the chaperonin cofactor Hsp10 for protein
1150 sorting in yeast mitochondria. *J Cell Biol/* 1994;126:305–315.
- 1151 24. Wu BJ, Morimoto RI. Transcription of the human hsp70 gene is induced by serum
1152 stimulation. *Proc Natl Acad Sci USA*. 1985;82: 6070-4.
- 1153 25. Ngr di A, Domoki F, Dgi R, Borda S, Pkski M, Szab A, Bari F. Up-regulation of
1154 cerebral carbonic anhydrase by anoxic stress in piglets. *J Neurochem*. 2003;85: 843-
1155 50.
- 1156 26. Lin KH, Kuo CH, Kuo WW, Ho TJ, Pai P, Chen WK, Pan LF, Wang CC, Padma VV,
1157 Huang CY. NFIL3 suppresses hypoxia-induced apoptotic cell death by targeting the
1158 insulin-like growth factor 2 receptor. *J Cell Biochem*. 2015;116: 1113-20. doi:
1159 10.1002/jcb.25067
- 1160 27. Zhang W, Zhang J, Kornuc M, Kwan K, Frank R, Nimer SD. Molecular cloning and
1161 characterization of NF-IL3A, a transcriptional activator of the human interleukin-3
1162 promoter. *Mol Cell Biol*. 1995;15: 6055-63.
- 1163 28. Smith TG, Robbins PA, Ratcliffe PJ. The human side of hypoxia-inducible factor. *Br*
1164 *J Haematol*. 2008, 141: 325-34. doi: 10.1111/j.1365-2141.2008.07029.x.
- 1165 29. Ino Y, Yamazaki-Itoh R, Oguro S, Shimada K, Kosuge T, Zavada J, Kanai Y,
1166 Hiraoka N. Arginase II expressed in cancer-associated fibroblasts indicates tissue
1167 hypoxia and predicts poor outcome in patients with pancreatic cancer. *PLoS One*.
1168 2013;8: e55146. doi: 10.1371/journal.pone.0055146.

- 1169 30. Lafleur VN, Richard S, Richard DE. Transcriptional repression of hypoxia-inducible
1170 factor-1 (HIF-1) by the protein arginine methyltransferase PRMT1. *Mol Biol Cell*.
1171 2014;25: 925-35. doi: 10.1091/mbc.E13-07-0423.
- 1172 31. Devlin CM, Lahm T, Hubbard WC, Van Demark M, Wang KC, Wu X, Bielawska A,
1173 Obeid LM, Ivan M, Petrache I. Dihydroceramide-based response to hypoxia. *J Biol*
1174 *Chem*. 2011;286: 38069-78. doi: 10.1074/jbc.M111.297994.
- 1175 32. Hannun YA, Obeid LM. Principles of bioactive lipid signalling: lessons from
1176 sphingolipids. *Nat Rev Mol Cell Biol*. 2008;9: 139-50. doi: 10.1038/nrm2329.
- 1177 33. Mao C, Obeid LM. Ceramidases: regulators of cellular responses mediated by
1178 ceramide, sphingosine, and sphingosine-1-phosphate. *Biochim Biophys Acta*.
1179 2008;1781: 424-34. doi: 10.1016/j.bbaliip.2008.06.002.
- 1180 34. Rhee SG, Chae HZ, Kim K. Peroxiredoxins: a historical overview and speculative
1181 preview of novel mechanisms and emerging concepts in cell signaling. *Free Radic*
1182 *Biol Med*. 2005;38: 1543-52.
- 1183 35. Salzano S, Checconi P, Hanschmann EM, Lillig CH, Bowler LD, Chan P, Vaudry D,
1184 Mengozzi M, Coppo L, Sacre S, Atkuri KR, Sahaf B, Herzenberg LA, Herzenberg
1185 LA, Mullen L, Ghezzi P. Linkage of inflammation and oxidative stress via release of
1186 glutathionylated peroxiredoxin-2, which acts as a danger signal. *Proc Natl Acad Sci*
1187 *USA*. 2014;111: 12157-62. doi: 10.1073/pnas.1401712111.
- 1188 36. Landau G, Ran A, Bercovich Z, Feldmesser E, Horn-Saban S, Korkotian E, Jacob-
1189 Hirsh J, Rechavi G, Ron D, Kahana C. Expression profiling and biochemical analysis
1190 suggest stress response as a potential mechanism inhibiting proliferation of
1191 polyamine-depleted cells. *J Biol Chem*. 2012; 287:35825-37. doi:
1192 10.1074/jbc.M112.381335.
- 1193 37. Fornace AJ Jr, Jackman J, Hollander MC, Hoffman-Liebermann B, Liebermann DA.
1194 Genotoxic-stress-response genes and growth-arrest genes. *gadd*, *MyD*, and other
1195 genes induced by treatments eliciting growth arrest. *Ann N Y Acad Sci*. 1992;663:
1196 139-53.
- 1197 38. Schmitz I. Gadd45 proteins in immunity. In: D.A. Liebermann and B. Hoffman (eds),
1198 *Gadd45 Stress Sensor Genes, Advances in Experimental Medicine and Biology 793*,
1199 Springer Science+Business Media New York 2013.
- 1200 39. Lisowski P, Wieczorek M, Goscik J, Juszczak GR, Stankiewicz AM, Zwierzchowski
1201 L, Swiergiel AH. Effects of chronic stress on prefrontal cortex transcriptome in mice
1202 displaying different genetic backgrounds. *J Mol Neurosci*. 2013;50: 33-57. doi:
1203 10.1007/s12031-012-9850-1.
- 1204 40. Timpl P, Spanagel R, Sillaber I, Kresse A, Reul JM, Stalla GK, Blanquet V, Steckler
1205 T, Holsboer F, Wurst W. Impaired stress response and reduced anxiety in mice
1206 lacking a functional corticotropin-releasing hormone receptor 1. *Nat Genet*. 1998;19:
1207 162-6.
- 1208 41. Leikauf GD, Concel VJ, Bein K, Liu P, Berndt A, Martin TM, Ganguly K, Jang AS,
1209 Brant KA, Dopico RA Jr, Upadhyay S, Cario C, Di YP, Vuga LJ, Kostem E, Eskin E,
1210 You M, Kaminski N, Prows DR, Knoell DL, Fabisiak JP. Functional genomic

- 1211 assessment of phosgene-induced acute lung injury in mice. *Am J Respir Cell Mol*
1212 *Biol.* 2013;49: 368-83. doi: 10.1165/rcmb.2012-0337OC.
- 1213 42. Nice TJ, Deng W, Coscoy L, Raulet DH. Stress-regulated targeting of the NKG2D
1214 ligand Mult1 by a membrane-associated RING-CH family E3 ligase. *J Immunol.*
1215 2010;185: 5369-76. doi: 10.4049/jimmunol.1000247.
- 1216 43. Kokame K, Agarwala KL, Kato H, Miyata T. Herp, a new ubiquitin-like membrane
1217 protein induced by endoplasmic reticulum stress. *J Biol Chem.* 2000;275: 32846-53.
- 1218 44. Coates PJ, Nenuil R, McGregor A, Picksley SM, Crouch DH, Hall PA, Wright EG.
1219 Mammalian prohibitin proteins respond to mitochondrial stress and decrease during
1220 cellular senescence. *Exp Cell Res.* 2001; 265:262-73.
- 1221 45. Wehner KA, Schtz S, Sarnow P. OGFOD1, a novel modulator of eukaryotic
1222 translation initiation factor 2alpha phosphorylation and the cellular response to stress.
1223 *Mol Cell Biol.* 2010;30: 2006-16. doi: 10.1128/MCB.01350-09.
- 1224 46. Rock KL, Lai JJ, Kono H. Innate and adaptive immune responses to cell death.
1225 *Immunol Rev.* 2011;243: 191-205. doi: 10.1111/j.1600-065X.2011.01040.x.
- 1226 47. Crist SA, Elzey BD, Ahmann MT, Ratliff TL. Early growth response-1 (EGR-1) and
1227 nuclear factor of activated T cells (NFAT) cooperate to mediate CD40L expression in
1228 megakaryocytes and platelets. *J Biol Chem.* 2013;288: 33985-96. doi:
1229 10.1074/jbc.M113.511881.
- 1230 48. Li S, Miao T, Sebastian M, Bhullar P, Ghaffari E, Liu M, Symonds AL, Wang P. The
1231 transcription factors Egr2 and Egr3 are essential for the control of inflammation and
1232 antigen-induced proliferation of B and T cells. *Immunity.* 2012;37: 685-96. doi:
1233 10.1016/j.immuni.2012.08.001.
- 1234 49. Jayaraman P, Sada-Ovalle I, Nishimura T, Anderson AC, Kuchroo VK, Remold HG,
1235 Behar SM. IL-1 β promotes antimicrobial immunity in macrophages by regulating
1236 TNFR signaling and caspase-3 activation. *J Immunol.* 2013;190: 4196-204. doi:
1237 10.4049/jimmunol.1202688.
- 1238 50. Hughes AL. Origin and diversification of the L-amino oxidase family in innate
1239 immune defenses of animals. *Immunogenetics.* 2010;62: 753-9. doi: 10.1007/s00251-
1240 010-0482-8.
- 1241 51. Ramirez-Carrozzi V, Sambandam A, Luis E, Lin Z, Jeet S, Lesch J, Hackney J, Kim
1242 J, Zhou M, Lai J, Modrusan Z, Sai T, Lee W, Xu M, Caplazi P, Diehl L, de Voss J,
1243 Balazs M, Gonzalez L Jr, Singh H, Ouyang W, Pappu R. IL-17C regulates the innate
1244 immune function of epithelial cells in an autocrine manner. *Nat Immunol.* 2011;12:
1245 1159-66 doi: 10.1038/ni.2156.
- 1246 52. Zuccolo J, Bau J, Childs SJ, Goss GG, Sensen CW, Deans JP. Phylogenetic analysis
1247 of the MS4A and TMEM176 gene families. *PLoS One.* 2010, 5: e9369. doi:
1248 10.1371/journal.pone.0009369.
- 1249 53. Allen A, Hutton DA, Pearson JP. The MUC2 gene product: a human intestinal mucin.
1250 *Int J Biochem Cell Biol.* 1998;30: 797-801.

- 1251 54. Michelucci A, Cordes T, Ghelfi J, Pailot A, Reiling N, Goldmann O, Binz T, Wegner
1252 A, Tallam A, Rausell A, Buttini M, Linster CL, Medina E, Balling R, Hiller K.
1253 Immune-responsive gene 1 protein links metabolism to immunity by catalyzing
1254 itaconic acid production. *Proc Natl Acad Sci USA*. 2013;110: 7820-5. doi:
1255 10.1073/pnas.1218599110.
- 1256 55. Honke N, Shaabani N, Cadeddu G, Sorg UR, Zhang DE, Trilling M, Klingel K,
1257 Sauter M, Kandolf R, Gailus N, van Rooijen N, Burkart C, Baldus SE, Grusdat M,
1258 Lhning M, Hengel H, Pfeffer K, Tanaka M, Hussinger D, Recher M, Lang PA, Lang
1259 KS. Enforced viral replication activates adaptive immunity and is essential for the
1260 control of a cytopathic virus. *Nat Immunol*. 2011;13: 51-7. doi: 10.1038/ni.2169.
- 1261 56. Martinez-Lpez M, Iborra S, Conde-Garrosa R, Sancho D. Batf3-dependent CD103+
1262 dendritic cells are major producers of IL-12 that drive local Th1 immunity against
1263 *Leishmania major* infection in mice. *Eur J Immunol*. 2015;45: 119-29. doi:
1264 10.1002/eji.201444651.
- 1265 57. Imai T, Baba M, Nishimura M, Kakizaki M, Takagi S, Yoshie O. The T cell-directed
1266 CC chemokine TARC is a highly specific biological ligand for CC chemokine
1267 receptor 4. *J Biol Chem*. 1997;272: 15036-42.
- 1268 58. Vong QP, Leung WH1, Houston J1, Li Y1, Rooney B1, Holladay M1, Oostendorp
1269 RA2, Leung W3. TOX2 regulates human natural killer cell development by
1270 controlling T-BET expression. *Blood*. 2014;124: 3905-13. doi: 10.1182/blood-2014-
1271 06-582965.
- 1272 59. Takaori A. Antiviral defense by APOBEC3 family proteins. *Uirusu*. 2005;55: 267-72.
- 1273 60. Arming S, Wipfler D, Mayr J, Merling A, Vilas U, Schauer R, Schwartz-Albiez R,
1274 Vlasak R. The human Cas1 protein: a sialic acid-specific O-acetyltransferase?
1275 *Glycobiology*. 2011;21: 553-64. doi: 10.1093/glycob/cwq153.
- 1276 61. Crocker PR, Paulson JC, Varki A. Siglecs and their roles in the immune system. *Nat*
1277 *Rev Immunol*. 2007;7: 255-66.
- 1278 62. Crocker PR, Varki A. Siglecs in the immune system. *Immunology*. 2001;103: 137-45.
- 1279 63. Shi WX, Chammas R, Varki NM, Powell L, Varki A. Sialic acid 9-O-acetylation on
1280 murine erythroleukemia cells affects complement activation, binding to I-type lectins,
1281 and tissue homing. *J Biol Chem*. 1996;271: 31526-32.
- 1282 64. Praper T, Sonnen A, Viero G, Kladnik A, Froelich CJ, Anderluh G, Dalla Serra M,
1283 Gilbert RJ. Human perforin employs different avenues to damage membranes. *J Biol*
1284 *Chem*. 2011;286: 2946-55. doi: 10.1074/jbc.M110.169417.
- 1285 65. Tschopp J, Masson D, Stanley KK. Structural/functional similarity between proteins
1286 involved in complement- and cytotoxic T-lymphocyte-mediated cytolysis. *Nature*.
1287 1986;322: 831-4.
- 1288 66. White SH, Wimley WC, Selsted ME. Structure, function, and membrane integration
1289 of defensins. *Curr Opin Struct Biol*. 1995;5: 521-7.
- 1290 67. Blanchong CA, Chung EK, Rupert KL, Yang Y, Yang Z, Zhou B, Moulds JM, Yu
1291 CY. Genetic, structural and functional diversities of human complement components

- 1292 C4A and C4B and their mouse homologues, Slp and C4. *Int Immunopharmacol.*
1293 2001;1: 365-92.
- 1294 68. Chen L, Carico Z, Shih HY, Krangel MS. A discrete chromatin loop in the mouse
1295 Tcr α -Tcr δ locus shapes the TCR δ and TCR α repertoires. *Nat Immunol.* 2015;16:
1296 1085-93. doi: 10.1038/ni.3232.
- 1297 69. Grage-Griebenow E, Flad HD, Ernst M, Bzowska M, Skrzeczyska J, Pryjma J.
1298 Human MO subsets as defined by expression of CD64 and CD16 differ in phagocytic
1299 activity and generation of oxygen intermediates. *Immunobiology.* 2000;202: 42-50.
- 1300 70. Al-Banna NA, Vaci M, Slauenwhite D, Johnston B, Issekutz TB. CCR4 and CXCR3
1301 play different roles in the migration of T cells to inflammation in skin, arthritic joints,
1302 and lymph nodes. *Eur J Immunol.* 2014;44: 1633-43. doi: 10.1002/eji.201343995.
1303 Epub 2014 Apr 23.
- 1304 71. Icutani M, Yanagibashi T, Ogasawara M, Tsuneyama K, Yamamoto S, Hattori Y,
1305 Kouro T, Itakura A, Nagai Y, Takaki S, Takatsu K. Identification of innate IL-5-
1306 producing cells and their role in lung eosinophil regulation and antitumor immunity. *J*
1307 *Immunol.* 2012;188: 703-13. doi: 10.4049/jimmunol.1101270. Epub 2011 Dec 14.
- 1308 72. Lillard JW Jr, Boyaka PN, Taub DD, McGhee JR. RANTES potentiates antigen-
1309 specific mucosal immune responses. *J Immunol.* 2001;166: 162-9.
- 1310 73. Kawasaki N, Rademacher C, Paulson JC. CD22 regulates adaptive and innate
1311 immune responses of B cells. *J Innate Immun.* 2011;3: 411-9. doi:
1312 10.1159/000322375.
- 1313 74. Liu H, Thaker YR, Stagg L, Schneider H, Ladbury JE, Rudd CE. SLP-76 sterile α
1314 motif (SAM) and individual H5 α helix mediate oligomer formation for microclusters
1315 and T-cell activation. *J Biol Chem.* 2013;288: 29539-49. doi:
1316 10.1074/jbc.M112.424846.
- 1317 75. Feeley EM, Sims JS, John SP, Chin CR, Pertel T, Chen LM, Gaiha GD, Ryan BJ,
1318 Donis RO, Elledge SJ, Brass AL. IFITM3 inhibits influenza A virus infection by
1319 preventing cytosolic entry. *PLoS Pathog.* 2011;7: e1002337. doi:
1320 10.1371/journal.ppat.1002337.
- 1321 76. Saben J, Zhong Y, Gomez-Acevedo H, Thakali KM, Borengasser SJ, Andres A,
1322 Shankar K. Early growth response protein-1 mediates lipotoxicity-associated
1323 placental inflammation: role in maternal obesity. *Am J Physiol Endocrinol Metab.*
1324 2013;305: e1-14. doi: 10.1152/ajpendo.00076.2013.
- 1325 77. Ren K, Torres R. Role of interleukin-1 β during pain and inflammation. *Brain Res*
1326 *Rev.* 2009;60: 57-64. doi: 10.1016/j.brainresrev.2008.12.020.
- 1327 78. Chen GY, Nuñez G. Sterile inflammation: sensing and reacting to damage. *Nat Rev*
1328 *Immunol.* 2010;10: 826-37. doi: 10.1038/nri2873.
- 1329 79. Sedger LM, McDermott MF. TNF and TNF-receptors: From mediators of cell death
1330 and inflammation to therapeutic giants - past, present and future. *Cytokine Growth*
1331 *Factor Rev.* 2014;25: 453-72. doi: 10.1016/j.cytogfr.2014.07.016.

- 1332 80. Lee TS, Chau LY. Heme oxygenase-1 mediates the anti-inflammatory effect of
1333 interleukin-10 in mice. *Nat Med.* 2002;8: 240-6.
- 1334 81. Piantadosi CA, Withers CM, Bartz RR, MacGarvey NC, Fu P, Sweeney TE, Welty-
1335 Wolf KE, Suliman HB. Heme oxygenase-1 couples activation of mitochondrial
1336 biogenesis to anti-inflammatory cytokine expression. *J Biol Chem.* 2011;286: 16374-
1337 85. doi: 10.1074/jbc.M110.207738.
- 1338 82. Guo Y, Zhang W, Giroux C, Cai Y, Ekambaram P, Dilly AK, Hsu A, Zhou S,
1339 Maddipati KR, Liu J, Joshi S, Tucker SC, Lee MJ, Honn KV. Identification of the
1340 orphan G protein-coupled receptor GPR31 as a receptor for 12-(S)-
1341 hydroxyeicosatetraenoic acid. *J Biol Chem.* 2011;286: 33832-40. doi:
1342 10.1074/jbc.M110.216564.
- 1343 83. Bickel M. The role of interleukin-8 in inflammation and mechanisms of regulation. *J*
1344 *Periodontol.* 1993;64: 456-60.
- 1345 84. Alcock J, Franklin ML, Kuzawa CW. Nutrient signaling: evolutionary origins of the
1346 immune-modulating effects of dietary fat. *Q Rev Biol* 2012;87: 187-223.
- 1347 85. Pearson G, Robinson F, Beers Gibson T, Xu BE, Karandikar M, Berman K, Cobb
1348 MH. Mitogen-activated protein (MAP) kinase pathways: regulation and physiological
1349 functions. *Endocr Rev.* 2001;22: 153-83.
- 1350 86. Tsatsanis C, Androulidaki A, Dermitzaki E, Gravanis A, Margioris AN. Corticotropin
1351 releasing factor receptor 1 (CRF1) and CRF2 agonists exert an anti-inflammatory
1352 effect during the early phase of inflammation suppressing LPS-induced TNF-alpha
1353 release from macrophages via induction of COX-2 and PGE2. *J Cell Physiol.*
1354 2007;210: 774-83.
- 1355 87. Frugier T, Morganti-Kossmann MC, O'Reilly D, McLean CA. In situ detection of
1356 inflammatory mediators in post mortem human brain tissue after traumatic injury. *J*
1357 *Neurotrauma.* 2010;27: 497-507. doi: 10.1089/neu.2009.1120.
- 1358 88. Sawant DV, Sehra S, Nguyen ET, Jadhav R, Englert K, Shinnakasu R, Hangoc G,
1359 Broxmeyer HE, Nakayama T, Perumal NB, Kaplan MH, Dent AL. Bcl6 controls the
1360 Th2 inflammatory activity of regulatory T cells by repressing Gata3 function. *J*
1361 *Immunol.* 2012;189: 4759-69. doi: 10.4049/jimmunol.1201794.
- 1362 89. Correa-Costa M, Andrade-Oliveira V, Braga TT, Castoldi A, Aguiar CF, Origassa
1363 CS2, Rodas AC, Hiyane MI, Malheiros DM, Rios FJ, Jancar S, Cmara NO.
1364 Activation of platelet-activating factor receptor exacerbates renal inflammation and
1365 promotes fibrosis. *Lab Invest.* 2014;94: 455-66. doi: 10.1038/labinvest.2013.155.
- 1366 90. Watson RP, Lilley E, Panesar M, Bhalay G, Langridge S, Tian SS, McClenaghan C,
1367 Ropenga A, Zeng F, Nash MS. Increased prokineticin 2 expression in gut
1368 inflammation: role in visceral pain and intestinal ion transport. *Neurogastroenterol*
1369 *Motil.* 2012;24: 65-75 doi: 10.1111/j.1365-2982.2011.01804.x.
- 1370 91. Pavlov VA, Wang H, Czura CJ, Friedman SG, Tracey KJ. The cholinergic anti-
1371 inflammatory pathway: a missing link in neuroimmunomodulation. *Mol Med.* 2003;9:
1372 125-34.

- 1373 92. Lerdrup M, Holmberg C, Dietrich N, Shaulian E, Herdegen T, Jttel M, Kallunki T.
1374 Depletion of the AP-1 repressor JDP2 induces cell death similar to apoptosis.
1375 *Biochim Biophys Acta*. 2005;1745: 29-37.
- 1376 93. Hu W, Xu R, Sun W, Szulc ZM, Bielawski J, Obeid LM, Mao C. Alkaline
1377 ceramidase 3 (ACER3) hydrolyzes unsaturated long-chain ceramides, and its down-
1378 regulation inhibits both cell proliferation and apoptosis. *J Biol Chem*. 2010;285:
1379 7964-76. doi: 10.1074/jbc.M109.063586.
- 1380 94. Preston GA, Lyon TT, Yin Y, Lang JE, Solomon G, Annab L, Srinivasan DG,
1381 Alcorta DA, Barrett JC. Induction of apoptosis by c-Fos protein. *Mol Cell Biol*.
1382 1996;16: 211-8.
- 1383 95. Adrain C, Creagh EM, Martin SJ. Apoptosis-associated release of Smac/DIABLO
1384 from mitochondria requires active caspases and is blocked by Bcl-2. *EMBO J*.
1385 2001;20: 6627-36.
- 1386 96. McNeish IA, Lopes R, Bell SJ, McKay TR, Fernandez M, Lockley M, Wheatley SP,
1387 Lemoine NR. Survivin interacts with Smac/DIABLO in ovarian carcinoma cells but
1388 is redundant in Smac-mediated apoptosis. *Exp Cell Res*. 2005;302: 69-82.
- 1389 97. Zhao F, Wang Q. The protective effect of peroxiredoxin II on oxidative stress
1390 induced apoptosis in pancreatic β -cells. *Cell Biosci*. 2012;2: 22. doi: 10.1186/2045-
1391 3701-2-22.
- 1392 98. Wu X, Hernandez-Enriquez B, Banas M, Xu R, Sesti F. Molecular mechanisms
1393 underlying the apoptotic effect of KCNB1 K⁺ channel oxidation. *J Biol Chem*.
1394 2013;288: 4128-34. doi: 10.1074/jbc.M112.440933.
- 1395 99. Tang D, Lahti JM, Kidd VJ. Caspase-8 activation and bid cleavage contribute to
1396 MCF7 cellular execution in a caspase-3-dependent manner during staurosporine-
1397 mediated apoptosis. *J Biol Chem*. 2000;275: 9303-7.
- 1398 100. Chinnadurai G, Vijayalingam S, Rashmi R. BIK, the founding member of the
1399 BH3-only family proteins: mechanisms of cell death and role in cancer and
1400 pathogenic processes. *Oncogene*. 2008;27: S20-9. doi: 10.1038/onc.2009.40.
- 1401 101. Iwasa H, Kudo T, Maimaiti S, Ikeda M, Maruyama J, Nakagawa K, Hata Y. The
1402 RASSF6 tumor suppressor protein regulates apoptosis and the cell cycle via MDM2
1403 protein and p53 protein. *J Biol Chem*. 2013;288:30320-9. doi:
1404 10.1074/jbc.M113.507384.
- 1405 102. Liu X, Dong C, Jiang Z, Wu WK, Chan MT, Zhang J, Li H, Qin K, Sun X.
1406 MicroRNA-10b downregulation mediates acute rejection of renal allografts by
1407 derepressing BCL2L11. *Exp Cell Res*. 2015;333: 155-63. doi:
1408 10.1016/j.yexcr.2015.01.018.
- 1409 103. Sayed M, Pelech S, Wong C, Marotta A, Salh B. Protein kinase CK2 is involved
1410 in G2 arrest and apoptosis following spindle damage in epithelial cells. *Oncogene*.
1411 2001;20: 6994-7005.
- 1412 104. Maddigan A, Truitt L, Arsenault R, Freywald T, Allonby O, Dean J, Narendran
1413 A, Xiang J, Weng A, Napper S, Freywald A. EphB receptors trigger Akt activation

- 1414 and suppress Fas receptor-induced apoptosis in malignant T lymphocytes. *J Immunol.*
1415 2011;187: 5983-94. doi: 10.4049/jimmunol.1003482.
- 1416 105. Okamoto S, Krainc D, Sherman K, Lipton SA. Antiapoptotic role of the p38
1417 mitogen-activated protein kinase-myocyte enhancer factor 2 transcription factor
1418 pathway during neuronal differentiation. *Proc Natl Acad Sci USA.* 2000;97: 7561-6.
- 1419 106. Chiorazzi M, Rui L, Yang Y, Ceribelli M, Tishbi N, Maurer CW, Ranuncolo SM,
1420 Zhao H, Xu W, Chan WC, Jaffe ES, Gascoyne RD, Campo E, Rosenwald A, Ott G,
1421 Delabie J, Rimsza LM, Shaham S, Staudt LM. Related F-box proteins control cell
1422 death in *Caenorhabditis elegans* and human lymphoma. *Proc Natl Acad Sci USA.*
1423 2013;110: 3943-8. doi: 10.1073/pnas.1217271110.
- 1424 107. Bloch DB, Nakajima A, Gulick T, Chiche JD, Orth D, de La Monte SM, Bloch
1425 KD. Sp110 localizes to the PML-Sp100 nuclear body and may function as a nuclear
1426 hormone receptor transcriptional coactivator. *Mol Cell Biol.* 2000;20: 6138-46.
- 1427 108. Bengoechea-Alonso MT, Ericsson J. Tumor suppressor Fbxw7 regulates TGF β
1428 signaling by targeting TGIF1 for degradation. *Oncogene.* 2010;29: 5322-8. doi:
1429 10.1038/onc.2010.278. Epub 2010 Jul 12.
- 1430 109. Ma Y, Wang B, Li W, Ying G, Fu L, Niu R, Gu F. Reduction of intersectin1-s
1431 induced apoptosis of human glioblastoma cells. *Brain Res.* 2010;1351: 222-8. doi:
1432 10.1016/j.brainres.2010.05.028.
- 1433 110. Gnesutta N, Qu J, Minden A. The serine/threonine kinase PAK4 prevents caspase
1434 activation and protects cells from apoptosis. *J Biol Chem.* 2001;276: 14414-9.
- 1435 111. Markovich D. Physiological roles and regulation of mammalian sulfate
1436 transporters. *Physiol Rev.* 2001;81: 1499-533.
- 1437 112. Guasti L, Crociani O, Redaelli E, Pillozzi S, Polvani S, Masselli M, Mello T,
1438 Galli A, Amedei A, Wymore RS, Wanke E, Arcangeli A. Identification of a
1439 posttranslational mechanism for the regulation of hERG1 K⁺ channel expression and
1440 hERG1 current density in tumor cells. *Mol Cell Biol.* 2008;28: 5043-60. doi:
1441 10.1128/MCB.00304-08.
- 1442 113. Bremser M, Nickel W, Schweikert M, Ravazzola M, Amherdt M, Hughes CA,
1443 Sllner TH, Rothman JE, Wieland FT. Coupling of coat assembly and vesicle budding
1444 to packaging of putative cargo receptors. *Cell.* 1999;96: 495-506.
- 1445 114. Zhen Y, Srensen V, Skjerpen CS, Haugsten EM, Jin Y, Wichli S, Olsnes S,
1446 Wiedlocha A. Nuclear import of exogenous FGF1 requires the ER-protein LRRC59
1447 and the importins Kpn α 1 and Kpn β 1. *Traffic.* 2012;13: 650-64. doi: 10.1111/j.1600-
1448 0854.2012.01341.x.
- 1449 115. Bangs P, Burke B, Powers C, Craig R, Purohit A, Doxsey S. Functional analysis
1450 of Tpr: identification of nuclear pore complex association and nuclear localization
1451 domains and a role in mRNA export. *J Cell Biol.* 1998;143: 1801-12.
- 1452 116. Nakielny S, Siomi MC, Siomi H, Michael WM, Pollard V, Dreyfuss G.
1453 Transportin: nuclear transport receptor of a novel nuclear protein import pathway.
1454 *Exp Cell Res.* 1996;229: 261-6.

- 1455 117. Chi NC, Adam EJ, Adam SA. Sequence and characterization of cytoplasmic
1456 nuclear protein import factor p97. *J Cell Biol.* 1995;130: 265-74.
- 1457 118. Tang BL, Low DY, Tan AE, Hong W. Syntaxin 10: a member of the syntaxin
1458 family localized to the trans-Golgi network. *Biochem Biophys Res Commun.*
1459 1998;242: 345-50.
- 1460 119. Chen G. Biochemical properties of urea transporters. *Subcell Biochem.* 2014;73:
1461 109-26. doi: 10.1007/978-94-017-9343-8_7. PMID: 25298341
- 1462 120. Palmieri L, Pardo B, Lasorsa FM, del Arco A, Kobayashi K, Iijima M, Runswick
1463 MJ, Walker JE, Saheki T, Satrstegui J, Palmieri F. Citrin and aralar1 are Ca(2+)-
1464 stimulated aspartate/glutamate transporters in mitochondria. *EMBO J.* 2001;20: 5060-
1465 9.
- 1466 121. Hatanaka T, Huang W, Ling R, Prasad PD, Sugawara M, Leibach FH, Ganapathy
1467 V. Evidence for the transport of neutral as well as cationic amino acids by ATA3, a
1468 novel and liver-specific subtype of amino acid transport system A. *Biochim Biophys*
1469 *Acta.* 2001;1510: 10-7.
- 1470 122. Conchon S, Cao X, Barlowe C, Pelham HR. Got1p and Sft2p: membrane proteins
1471 involved in traffic to the Golgi complex. *EMBO J.* 1999;18: 3934-46.
- 1472 123. Hautbergue GM, Hung ML, Walsh MJ, Snijders AP, Chang CT, Jones R, Ponting
1473 CP, Dickman MJ, Wilson SA. UIF, a New mRNA export adaptor that works together
1474 with REF/ALY, requires FACT for recruitment to mRNA. *Curr Biol.* 2009;19: 1918-
1475 24. doi: 10.1016/j.cub.2009.09.041.
- 1476 124. Grempler R, Augustin R, Froehner S, Hildebrandt T, Simon E, Mark M,
1477 Eickelmann P. Functional characterisation of human SGLT-5 as a novel kidney-
1478 specific sodium-dependent sugar transporter. *FEBS Lett.* 2012;586: 248-53. doi:
1479 10.1016/j.febslet.2011.12.027.
- 1480 125. Dietmeier K, Hönlinger A, Bömer U, Dekker PJ, Eckerskorn C, Lottspeich F,
1481 Kübrich M, Pfanner N. Tom5 functionally links mitochondrial preprotein receptors to
1482 the general import pore. *Nature.* 1997;388: 195-200.
- 1483 126. Annilo T, Shulenin S, Chen ZQ, Arnould I, Prades C, Lemoine C, Maintoux-
1484 Larois C, Devaud C, Dean M, Denfle P, Rosier M. Identification and characterization
1485 of a novel ABCA subfamily member, ABCA12, located in the lamellar ichthyosis
1486 region on 2q34. *Cytogenet Genome Res.* 2002;98: 169-76.
- 1487 127. Moraes LA, Piqueras L, Bishop-Bailey D. Peroxisome proliferator-activated
1488 receptors and inflammation. *Pharmacol Ther.* 2006;110: 371-85.
- 1489 128. Allikmets R, Gerrard B, Hutchinson A, Dean M. Characterization of the human
1490 ABC superfamily: isolation and mapping of 21 new genes using the expressed
1491 sequence tags database. *Hum Mol Genet.* 1996;5: 1649-55.
- 1492 129. Chew CS, Parente JA Jr, Chen X, Chaponnier C, Cameron RS. The LIM and SH3
1493 domain-containing protein, lasp-1, may link the cAMP signaling pathway with
1494 dynamic membrane restructuring activities in ion transporting epithelia. *J Cell Sci.*
1495 2000;113: 2035-45.

- 1496 130. Phillips-Krawczak CA, Singla A, Starokadomskyy P, Deng Z, Osborne DG, Li H,
1497 Dick CJ, Gomez TS, Koenecke M, Zhang JS, Dai H, Sifuentes-Dominguez L2, Geng
1498 LN, Kaufmann SH, Hein MY, Wallis M, McGaughran J, Gecz J, Sluis Bv, Billadeau
1499 DD, Burstein E. COMMD1 is linked to the WASH complex and regulates endosomal
1500 trafficking of the copper transporter ATP7A. *Mol Biol Cell*. 2015;26: 91-103. doi:
1501 10.1091/mbc.E14-06-1073.
- 1502 131. Tyson JR, Stirling CJ. LHS1 and SIL1 provide a luminal function that is essential
1503 for protein translocation into the endoplasmic reticulum. *EMBO J*. 2000;19: 6440-52.
- 1504 132. Sirrenberg C, Bauer MF, Guiard B, Neupert W, Brunner M. Import of carrier
1505 proteins into the mitochondrial inner membrane mediated by Tim22. *Nature*.
1506 1996;384: 582-5.
- 1507 133. Rubino M, Miaczynska M, Lipp R, Zerial M. Selective membrane recruitment of
1508 EEA1 suggests a role in directional transport of clathrin-coated vesicles to early
1509 endosomes. *J Biol Chem*. 2000;275: 3745-8.
- 1510 134. Zhu XR, Netzer R, Bhlke K, Liu Q, Pongs O. Structural and functional
1511 characterization of Kv6.2 a new gamma-subunit of voltage-gated potassium channel.
1512 *Receptors Channels*. 1999;6: 337-50.
- 1513 135. Toyama R, Kobayashi M, Tomita T, Dawid IB. Expression of LIM-domain
1514 binding protein (ldb) genes during zebrafish embryogenesis. *Mech Dev*. 1998;71:
1515 197-200.
- 1516 136. Kida YS, Sato T, Miyasaka KY, Suto A, Ogura T. Daam1 regulates the
1517 endocytosis of EphB during the convergent extension of the zebrafish notochord.
1518 *Proc Natl Acad Sci USA*. 2007;104: 6708-13.
- 1519 137. Gilpin BJ, Loechel F, Mattei MG, Engvall E, Albrechtsen R, Wewer UM. A
1520 novel, secreted form of human ADAM 12 (meltrin alpha) provokes myogenesis in
1521 vivo. *J Biol Chem*. 1998;273: 157-66.
- 1522 138. Sano K, Inohaya K, Kawaguchi M, Yoshizaki N, Iuchi I, Yasumasu S.
1523 Purification and characterization of zebrafish hatching enzyme - an evolutionary
1524 aspect of the mechanism of egg envelope digestion. *FEBS J*. 2008;275: 5934-46. doi:
1525 10.1111/j.1742-4658.2008.06722.x.
- 1526 139. Hofmeister-Brix A, Kollmann K, Langer S, Schultz J, Lenzen S, Baltrusch S.
1527 Identification of the ubiquitin-like domain of midnolin as a new glucokinase
1528 interaction partner. *J Biol Chem*. 2013;288: 35824-39. doi:
1529 10.1074/jbc.M113.526632.
- 1530 140. Tsukahara M, Suemori H, Noguchi S, Ji ZS, Tsunoo H. Novel nucleolar protein,
1531 midnolin, is expressed in the mesencephalon during mouse development. *Gene*.
1532 2000;254: 45-55.
- 1533 141. Hong SK, Dawid IB. FGF-dependent left-right asymmetry patterning in zebrafish
1534 is mediated by *Ier2* and *Fibp1*. *Proc Natl Acad Sci USA*. 2009;106: 2230-5. doi:
1535 10.1073/pnas.0812880106.

- 1536 142. Kwong RW, Perry SF. The tight junction protein claudin-b regulates epithelial
1537 permeability and sodium handling in larval zebrafish, *Danio rerio*. *Am J Physiol*
1538 *Regul Integr Comp Physiol* 2013;304: R504-13. doi: 10.1152/ajpregu.00385.2012.
- 1539 143. Ing T, Aoki Y. Expression of RGS2, RGS4 and RGS7 in the developing postnatal
1540 brain. *Eur J Neurosci*. 2002;15: 929-36.
- 1541 144. Wu T, Patel H, Mukai S, Melino C, Garg R, Ni X, Chang J, Peng C. Activin,
1542 inhibin, and follistatin in zebrafish ovary: expression and role in oocyte maturation.
1543 *Biol Reprod*. 2000;62: 1585-92.
- 1544 145. Malinauskas T, Aricescu AR, Lu W, Siebold C, Jones EY. Modular mechanism
1545 of Wnt signaling inhibition by Wnt inhibitory factor 1. *Nat Struct Mol Biol*. 2011;18:
1546 886-93. doi: 10.1038/nsmb.2081.
- 1547 146. Zagon IS, Wu Y, McLaughlin PJ. Opioid growth factor and organ development in
1548 rat and human embryos. *Brain Res*. 1999;839: 313-22.
- 1549 147. Takano A, Zochi R, Hibi M, Terashima T, Katsuyama Y. Expression of
1550 strawberry notch family genes during zebrafish embryogenesis. *Dev Dyn*. 2010;239:
1551 1789-96. doi: 10.1002/dvdy.22287.
- 1552 148. Pierani A, Moran-Rivard L, Sunshine MJ, Littman DR, Goulding M, Jessell TM.
1553 Control of interneuron fate in the developing spinal cord by the progenitor
1554 homeodomain protein *Dbx1*. *Neuron*. 2001;29: 367-84.
- 1555 149. Buonamici S, Chakraborty S, Senyuk V, Nucifora G. The role of EVI1 in normal
1556 and leukemic cells. *Blood Cells Mol Dis*. 2003;31: 206-12.
- 1557 150. Litwack ED, Babey R, Buser R, Gesemann M, O'Leary DD. Identification and
1558 characterization of two novel brain-derived immunoglobulin superfamily members
1559 with a unique structural organization. *Mol Cell Neurosci*. 2004;25: 263-74.
- 1560 151. Gazit R, Mandal PK, Ebina W, Ben-Zvi A, Nombela-Arrieta C, Silberstein LE,
1561 Rossi DJ. *Fgd5* identifies hematopoietic stem cells in the murine bone marrow. *J Exp*
1562 *Med*. 2014; 211: 1315-31. doi: 10.1084/jem.20130428.
- 1563 152. Zhang J, Tomasini AJ, Mayer AN. *RBM19* is essential for preimplantation
1564 development in the mouse. *BMC Dev Biol*. 2008;8: 115. doi: 10.1186/1471-213X-8-
1565 115.
- 1566 153. Tang K, Xie X, Park JI, Jamrich M, Tsai S, Tsai MJ. COUP-TFs regulate eye
1567 development by controlling factors essential for optic vesicle morphogenesis.
1568 *Development*. 2010;137: 725-34. doi: 10.1242/dev.040568.
- 1569 154. Zhang P, Bennoun M, Gogard C, Bossard P, Leclerc I, Kahn A, Vasseur-Cognet
1570 M. Expression of COUP-TFII in metabolic tissues during development. *Mech Dev*.
1571 2002;119: 109-14.
- 1572 155. Coumailleau P, Duprez D. *Sim1* and *Sim2* expression during chick and mouse
1573 limb development. *Int J Dev Biol*. 2009;53: 149-57. doi: 10.1387/ijdb.082659pc.
- 1574 156. Kondou H, Kawai M, Tachikawa K, Kimoto A, Yamagata M, Koinuma T,
1575 Yamazaki M, Nakayama M, Mushiake S, Ozono K, Michigami T. Sodium-coupled

- 1576 neutral amino acid transporter 4 functions as a regulator of protein synthesis during
1577 liver development. *Hepatol Res.* 2013;43: 1211-23. doi: 10.1111/hepr.12069.
- 1578 157. Li Z, Lai G, Deng L, Han Y, Zheng D, Song W. Association of SLC38A4 and
1579 system A with abnormal fetal birth weight. *Exp Ther Med.* 2012;3: 309-313.
- 1580 158. Tiberi L, van den Aemele J, Dimidschstein J, Piccirilli J, Gall D, Herpoel A,
1581 Bilheu A, Bonnefont J, Iacovino M, Kyba M, Bouschet T, Vanderhaeghen P. BCL6
1582 controls neurogenesis through Sirt1-dependent epigenetic repression of selective
1583 Notch targets. *Nat Neurosci.* 2012;15: 1627-35. doi: 10.1038/nn.3264.
- 1584 159. Matsuoka RL, Sun LO, Katayama K, Yoshida Y, Kolodkin AL. *Sema6B*,
1585 *Sema6C*, and *Sema6D* expression and function during mammalian retinal
1586 development. *PLoS One.* 2013;8: e63207. doi: 10.1371/journal.pone.0063207.
- 1587 160. Tamada H, Sakashita E, Shimazaki K, Ueno E, Hamamoto T, Kagawa Y, Endo H.
1588 cDNA cloning and characterization of *Drb1*, a new member of RRM-type neural
1589 RNA-binding protein. *Biochem Biophys Res Commun.* 2002;297: 96-104.
- 1590 161. Rempel RE, Saenz-Robles MT, Storms R, Morham S, Ishida S, Engel A, Jakoi L,
1591 Melhem MF, Pipas JM, Smith C, Nevins JR. Loss of E2F4 activity leads to abnormal
1592 development of multiple cellular lineages. *Mol Cell.* 2000;6: 293-306.
- 1593 162. Miyares RL, Stein C, Renisch B, Anderson JL, Hammerschmidt M, Farber SA.
1594 Long-chain Acyl-CoA synthetase 4A regulates Smad activity and dorsoventral
1595 patterning in the zebrafish embryo. *Dev Cell.* 2013;27: 635-47. doi:
1596 10.1016/j.devcel.2013.11.011.
- 1597 163. Louryan S, Biermans J, Flemal F. Nerve growth factor in the developing
1598 craniofacial region of the mouse embryo. *Eur J Morphol.* 1995;33: 415-9.
- 1599 164. Ko JA, Gondo T, Inagaki S, Inui M. Requirement of the transmembrane
1600 semaphorin *Sema4C* for myogenic differentiation. *FEBS Lett.* 2005;579: 2236-42.
- 1601 165. Wu H, Fan J, Zhu L, Liu S, Wu Y, Zhao T, Wu Y, Ding X, Fan W, Fan M.
1602 *Sema4C* expression in neural stem/progenitor cells and in adult neurogenesis induced
1603 by cerebral ischemia. *J Mol Neurosci.* 2009;39: 27-39. doi: 10.1007/s12031-009-
1604 9177-8.
- 1605 166. Pathirage NA, Cocquebert M, Sadovsky Y, Abumaree M, Manuelpillai U, Borg
1606 A, Keogh RJ, Brennecke SP, Evain-Brion D, Fournier T, Kalionis B, Murthi P.
1607 Homeobox gene transforming growth factor β -induced factor-1 (TGIF-1) is a
1608 regulator of villous trophoblast differentiation and its expression is increased in
1609 human idiopathic fetal growth restriction. *Mol Hum Reprod.* 2013;19: 665-75. doi:
1610 10.1093/molehr/gat042.
- 1611 167. Heger S, Mastronardi C, Dissen GA, Lomniczi A, Cabrera R, Roth CL, Jung H,
1612 Galimi F, Sippell W, Ojeda SR. Enhanced at puberty 1 (EAP1) is a new
1613 transcriptional regulator of the female neuroendocrine reproductive axis. *J Clin*
1614 *Invest.* 2007;117: 2145-54.
- 1615 168. Miao H, Strebhardt K, Pasquale EB, Shen TL, Guan JL, Wang B. Inhibition of
1616 integrin-mediated cell adhesion but not directional cell migration requires catalytic

- 1617 activity of EphB3 receptor tyrosine kinase. Role of Rho family small GTPases. *J Biol*
1618 *Chem.* 2005;280: 923-32.
- 1619 169. Vogel T, Boettger-Tong H, Nanda I, Dechend F, Agulnik AI, Bishop CE, Schmid
1620 M, Schmidtke J. A murine TSPY. *Chromosome Res.* 1998;6: 35-40.
- 1621 170. Janesick A, Shiotsugu J, Taketani M, Blumberg B. RIPPLY3 is a retinoic acid-
1622 inducible repressor required for setting the borders of the pre-placodal ectoderm.
1623 *Development.* 2012;139: 1213-24. doi: 10.1242/dev.071456.
- 1624 171. Zhou L, Zhang Z, Zheng Y, Zhu Y, Wei Z, Xu H, Tang Q, Kong X, Hu L.
1625 SKAP2, a novel target of HSF4b, associates with NCK2/F-actin at membrane ruffles
1626 and regulates actin reorganization in lens cell. *J Cell Mol Med.* 2011;15: 783-95. doi:
1627 10.1111/j.1582-4934.2010.01048.x.
- 1628 172. Wittschieben J, Shivji MK, Lalani E, Jacobs MA, Marini F, Gearhart PJ,
1629 Rosewell I, Stamp G, Wood RD. Disruption of the developmentally regulated Rev3l
1630 gene causes embryonic lethality. *Curr Biol.* 2000;10: 1217-20.
- 1631 173. Selvaraj A, Prywes R. Megakaryoblastic leukemia-1/2, a transcriptional co-
1632 activator of serum response factor, is required for skeletal myogenic differentiation. *J*
1633 *Biol Chem.* 2003;278: 41977-87.
- 1634 174. O'Shaughnessy RF, Welti JC, Sully K, Byrne C. Akt-dependent Pp2a activity is
1635 required for epidermal barrier formation during late embryonic development.
1636 *Development.* 2009;136: 3423-31. doi: 10.1242/dev.037010.
- 1637 175. Jaenisch R, Bird A. Epigenetic regulation of gene expression: how the genome
1638 integrates intrinsic and environmental signals. *Nat Genet.* 2003;33: 245-54.
- 1639 176. Gräff J, Kim D, Dobbin MM, Tsai LH. Epigenetic regulation of gene expression in
1640 physiological and pathological brain processes. *Physiol Rev.* 2011; 91: 603-49. doi:
1641 10.1152/physrev.00012.2010.
- 1642 177. Pan J, Jin C, Murata T, Yokoyama KK. Histone modification activities of JDP2
1643 associated with retinoic acid-induced differentiation of F9 cells. *Nucleic Acids*
1644 *Symp Ser (Oxf).* 2004;48: 189-90.
- 1645 178. Bowen NJ, Fujita N, Kajita M, Wade PA. Mi-2/NuRD: multiple complexes for
1646 many purposes. *Biochim Biophys Acta.* 2004;1677: 52-7.
- 1647 179. Sugimoto N, Maehara K, Yoshida K, Yasukouchi S, Osano S, Watanabe S, Aizawa
1648 M, Yugawa T, Kiyono T, Kurumizaka H, Ohkawa Y, Fujita M. Cdt1-binding
1649 protein GRWD1 is a novel histone-binding protein that facilitates MCM loading
1650 through its influence on chromatin architecture. *Nucleic Acids Res.* 2015;43: 5898-
1651 911. doi: 10.1093/nar/gkv509.
- 1652 180. Mariño-Ramírez L1, Kann MG, Shoemaker BA, Landsman D. Histone structure
1653 and nucleosome stability. *Expert Rev Proteomics.* 2005;2: 719-29.
- 1654 181. Yap KL, Li S, Muñoz-Cabello AM, Raguz S, Zeng L, Mujtaba S, Gil J, Walsh MJ,
1655 Zhou MM. Molecular interplay of the noncoding RNA ANRIL and methylated
1656 histone H3 lysine 27 by polycomb CBX7 in transcriptional silencing of INK4a.
1657 *Mol Cell.* 2010;38: 662-74. doi: 10.1016/j.molcel.2010.03.021.

- 1658 182. Ikegamii K, Horigome D, Mukai M, Livnat I, MacGregor GR, Setou M. TTL10
1659 is a protein polyglycyclase that can modify nucleosome assembly protein 1. FEBS
1660 Lett. 2008;582: 1129-34. doi: 10.1016/j.febslet.2008.02.079.
- 1661 183. Marzluff WF, Gongidi P, Woods KR, Jin J, Maltais LJ. The human and mouse
1662 replication-dependent histone genes. Genomics. 2002;80: 487-98.
- 1663 184. Li Y, Wen H, Xi Y, Tanaka K, Wang H, Peng D, Ren Y, Jin Q, Dent SY, Li W,
1664 Li H, Shi X. AF9 YEATS domain links histone acetylation to DOT1L-mediated
1665 H3K79 methylation. Cell. 2014;159: 558-71. doi: 10.1016/j.cell.2014.09.049.
- 1666 185. Iizuka M, Stillman B. Histone acetyltransferase HBO1 interacts with the ORC1
1667 subunit of the human initiator protein. J Biol Chem. 1999;274: 23027-34.
- 1668 186. Katoh M, Katoh M. Comparative integromics on JMJD1C gene encoding histone
1669 demethylase: conserved POU5F1 binding site elucidating mechanism of JMJD1C
1670 expression in undifferentiated ES cells and diffuse-type gastric cancer. Int J Oncol.
1671 2007;31: 219-23.
- 1672 187. González-Herrera L, Valenzuela A, Marchal JA, Lorente JA, Villanueva E. Studies
1673 on RNA integrity and gene expression in human myocardial tissue, pericardial fluid
1674 and blood, and its postmortem stability. Forensic Sci Int. 2013; 232: 218-28.
- 1675 188. Coyle RC, Latimer A, Jessen JR. Membrane-type 1 matrix metalloproteinase
1676 regulates cell migration during zebrafish gastrulation: evidence for an interaction
1677 with non-canonical Wnt signaling. Exp Cell Res. 2008;314: 2150-62. doi:
1678 10.1016/j.yexcr.2008.03.010.
- 1679 189. Gérard A, Patino-Lopez G, Beemiller P, Nambiar R, Ben-Aissa K, Liu Y, Totah FJ,
1680 Tyska MJ, Shaw S, Krummel MF. Detection of rare antigen-presenting cells
1681 through T cell-intrinsic meandering motility, mediated by *Myo1g*. Cell. 2014;15:
1682 492-505. doi: 10.1016/j.cell.2014.05.044.
- 1683 190. Müller T, Rumpel E, Hradetzky S, Bollig F, Wegner H, Blumenthal A, Greinacher
1684 A, Endlich K, Endlich N. Non-muscle myosin IIA is required for the development
1685 of the zebrafish glomerulus. Kidney Int. 2011;80: 1055-63. doi:
1686 10.1038/ki.2011.256.
- 1687 191. Ang Peng Hwa, Tekwani Shyam, Wang Guozhen. Shutting down the mobile phone
1688 and the downfall of Nepalese society, economy and politics. Pacific Affairs. 2012,
1689 85: 547-561.
- 1690 192. Sauer Hanno. Can't We All Disagree More Constructively? Moral Foundations,
1691 Moral Reasoning, and Political Disagreement. Neuroethics. 2015, 8: 153-169.
- 1692 193. Pahwa S, Scoglio C, Scala A. Abruptness of cascade failures in power grids. Sci
1693 Rep. 2014, 4: 3694. doi: 10.1038/srep03694.
- 1694 194. Mattson MP, Chan SL. Calcium orchestrates apoptosis. Nat Cell Biol. 2003, 5:
1695 1041-3.
- 1696 195. Lang F, Föller M, Lang KS, Lang PA, Ritter M, Gulbins E, Vereninov A, Huber
1697 SM. Ion channels in cell proliferation and apoptotic cell death. J Membr Biol. 2005,
1698 205: 147-57.

- 1699 196. Kauffman, Stuart A. The origins of order: self-organization and selection in
1700 evolution. New York: Oxford University Press; 1993.
- 1701 197. Tu Y, Stolovitzky G, Klein U. Quantitative noise analysis for gene expression
1702 microarray experiments. Proc Natl Acad Sci USA. 2002, 99: 14031.
- 1703 198. Jackson ES, Wayland MT, Fitzgerald W, Bahn S. A microarray data analysis
1704 framework for postmortem tissues. Methods 2005, 37: 247-60.
- 1705 199. Barash Y, Dehan E, Krupsky M, Franklin W, Geraci M, Friedman N, Kaminski N.
1706 Comparative analysis of algorithms for signal quantitation from oligonucleotide
1707 microarrays. Bioinform. 2004, 20: 839.
- 1708 200. Seo J, Bakay M, Chen YW, Hilmer S, Shneiderman B, Hoffman EP. Interactively
1709 optimizing signal-to-noise ratios in expression profiling: project-specific algorithm
1710 selection and detection p-value weighting in Affymetrix microarrays. Bioinform.
1711 2004, 20: 2534.
- 1712 201. Harr B, Schlötterer C, Comparison of algorithms for the analysis of Affymetrix
1713 microarray data as evaluated by co-expression of genes in known operons. Nucl
1714 Acids Res. 2006, 34: e8.
- 1715 202. Millenaar FF, Okyere J, May ST, van Zanten M, Voesenek LA, Peeters AJ. How to
1716 decide? Different methods of calculating gene expression from short
1717 oligonucleotide array data will give different results. BMC Bioinform. 2006, 7:
1718 137.
- 1719 203. Amend AS, Seifert KA, Bruns TD. Quantifying microbial communities with 454
1720 pyrosequencing: does read abundance count? Mol Ecol. 2010, 19: 5555.
- 1721 204. Aberg F, Pukkala E, Höckerstedt K, Sankila R, Isoniemi H. Risk of malignant
1722 neoplasms after liver transplantation: a population-based study. Liver Transpl.
1723 2008, 14: 1428-36.
- 1724 205. Haagsma EB, Hagens VE, Schaapveld M, van den Berg AP, de Vries EG,
1725 Klompaker IJ, Slooff MJ, Jansen PL. Increased cancer risk after liver
1726 transplantation: a population-based study. J Hepatol. 2001, 34: 84-91.

1727

Additional Files

Thanatotranscriptome: genes actively expressed after organismal death

Alex E. Pozhitkov, Rafik Neme, Tomislav Domazet-Lošo, Brian G. Leroux, Shivani Soni, Diethard Tautz and Peter A. Noble*.

*Correspondence to: panoble@washington.edu

This PDF file includes:

Supplementary Text

Figs S1, S2 and S3

Table S1

Other Additional Files for this manuscript include the following:

Data files S1 to S8 as zipped archives:

File S1. MiceProbesParameters.txt

File S2. FishProbesParameters.txt

File S3. Mouse_liver_Log10_AllProfiles.txt

File S4. Mouse_brain_Log10_AllProfiles.txt

File S5. Fish_Log10_AllProfiles.txt

File S6. MiceProbesSeq.txt

File S7. FishProbesSeq.txt

File S8. Gene_annotation_lit_refs_v3.xls

SUPPLEMENTARY TEXT

Fig S1. Bioanalyzer results showing total mRNA from the zebrafish.

Fig S2. Bioanalyzer results showing total mRNA from the mouse.

Fig S3. Transcriptional profiles in the zebrafish (*Acer3* gene) and mouse (*Cdc42* and *Rbm45* genes) by postmortem time.

Table S1. Total mRNA extracted (ng/ μ l tissue extract) from zebrafish by time and replicate sample.

Table S2. Total mRNA extracted (ng/ μ l tissue extract) from mouse organ/tissue by time and replicate sample.

Table S3. % of global regulator genes and response genes.

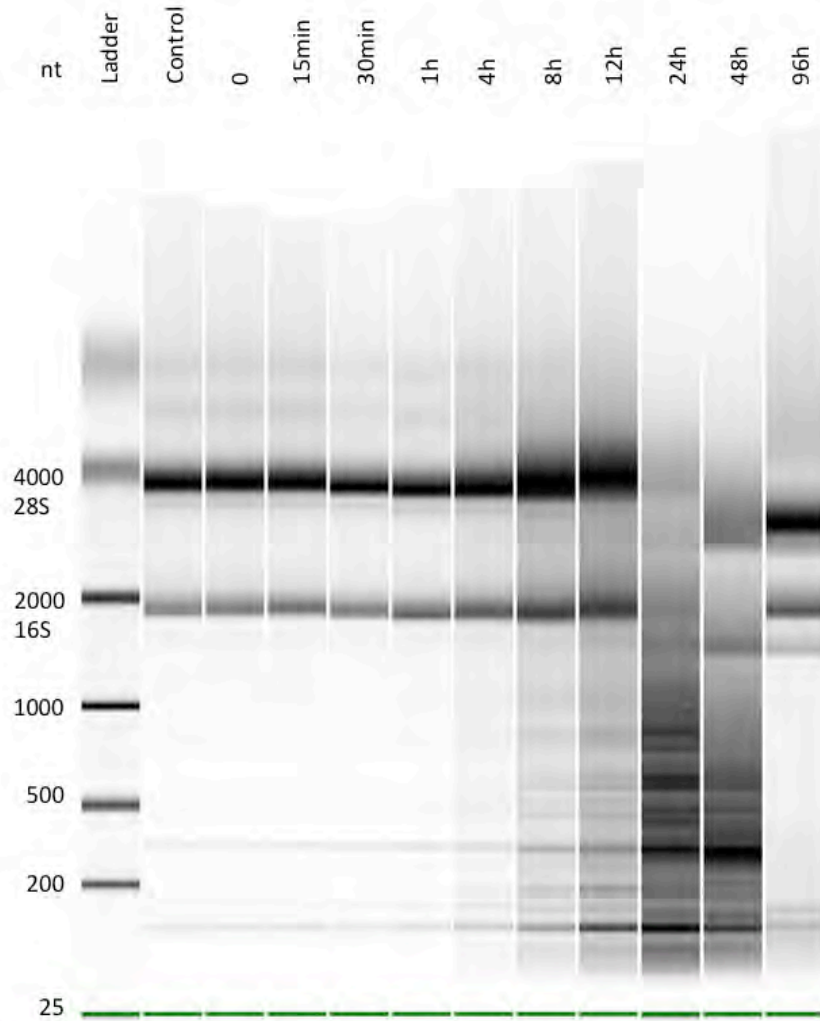


Fig S1. Bioanalyzer results showing total mRNA from the zebrafish. Only one replicate per sampling time is shown. The dominant bands represent the 28S and 18S rRNAs.

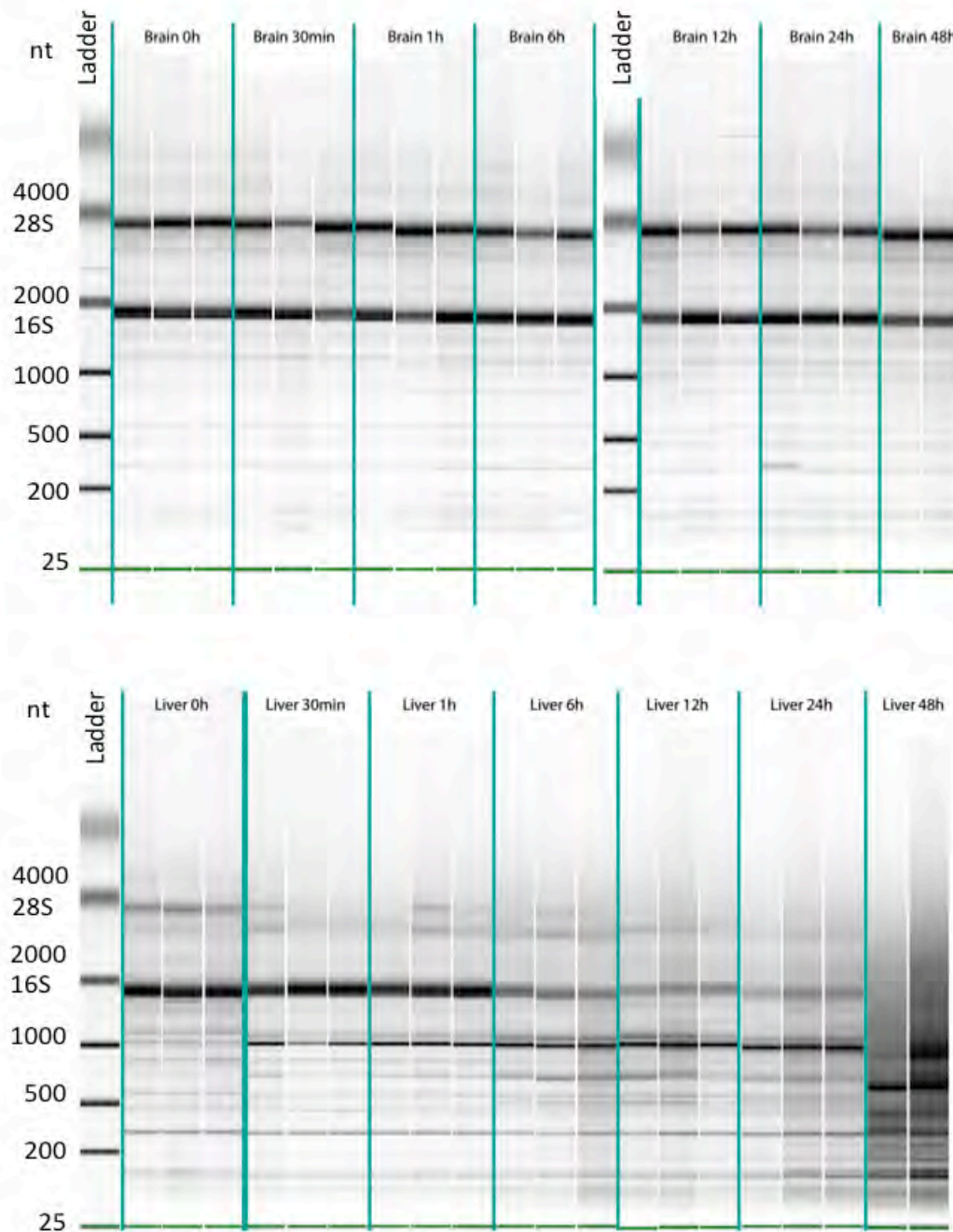


Fig S2. Bioanalyzer results showing total mRNA from the mouse. All replicates per sampling time are shown. The dominant bands represent the 28S and 18S rRNAs.

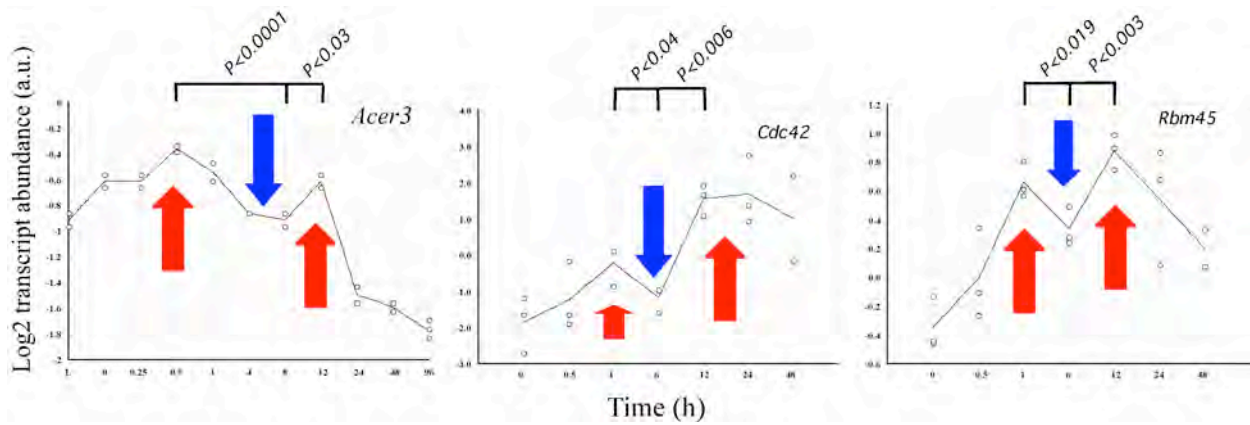


Fig S3. Transcriptional profiles in the zebrafish (*Acer3* gene) and mouse (*Cdc42* and *Rbm45* genes) by postmortem time. Red arrows, up-regulation; blue arrows, down-regulation. One-way T-tests show significant differences between means. Results suggest that the differences in up- and down regulation by postmortem time are due to changes in regulation rather than changes in “residual transcription levels”.

Table S1. Total mRNA extracted (ng/ μ l tissue extract) from zebrafish by time and replicate sample.

Time (h)	Repl#1	Repl#2
Live	1606	1648
0	1632	1481
0.25	1768	1573
0.5	1457	1481
1	1864	1514
4	1251	1651
8	1605	1499
12	1365	1422
24	1087	539
48	339	428
96	183	183

a, no replicate taken

Table S2. Total mRNA extracted (ng/ μ l tissue extract) from mouse organ/tissue by time and replicate sample.

Organ	Time (h)	Repl#1	Repl#2	Repl#3
Liver	0	432	387	443
Liver	0.5	533	651	569
Liver	1	421	426	601
Liver	6	541	624	528
Liver	12	839	450	845
Liver	24	1021	510	1066
Liver	48	1453	1197	- ^a
Brain	0	169	226	210
Brain	0.5	174	166	410
Brain	1	194	485	264
Brain	6	401	269	256
Brain	12	379	258	203
Brain	24	249	324	400
Brain	48	397	310	-

a, no replicate taken

Table S3. % of global regulator genes and response genes. Approx. 33% of all upregulated genes are involved in global regulation.

Global gene regulators and other response genes	Zebrafish	Mouse	Combined
Transcription factors and transcriptional regulatory genes	17	12	14
Cell signaling genes	24	16	19
Other response genes	59	73	67